Atmos. Meas. Tech. Discuss., doi:10.5194/amt-2016-227, 2016
Manuscript under review for journal Atmos. Meas. Tech.
Published: 29 August 2016

Atmospheric Measurement Techniques Discussions

Comparisons of the Orbiting Carbon Observatory-2 (OCO-2) X_{CO_2} measurements with TCCON

Debra Wunch[1,12], Paul O. Wennberg[1], Gregory Osterman[2,1], Brendan Fisher[2,1], Bret Naylor[2,1], Coleen M. Roehl[1], Christopher O'Dell[3], Lukas Mandrake[2,1], Camille Viatte[1], David W. T. Griffith[4], Nicholas M. Deutscher[4,5], Voltaire A. Velazco[4], Justus Notholt[5], Thorsten Warneke[5], Christof Petri[5], Martine De Maziere[6], Mahesh K. Sha[6], Ralf Sussmann[7], Markus Rettinger[7], David Pollard[8], John Robinson[8], Isamu Morino[9], Osamu Uchino[9], Frank Hase[10], Thomas Blumenstock[10], Matthaeus Kiel[10], Dietrich G. Feist[11], Sabrina G. Arnold[11], Kimberly Strong[12], Joseph Mendonca[12], Rigel Kivi[13], Pauli Heikkinen[13], Laura Iraci[14], James Podolske[14], Patrick W. Hillyard[14,19], Shuji Kawakami[15], Manvendra K. Dubey[16], Harrison A. Parker[16], Eliezer Sepulveda[17], Omaira E. G. Rodriguez[17], Yao Te[18], Pascal Jeseck[18], Michael R. Gunson[2,1], David Crisp[2,1], and Annmarie Eldering[2,1]

[1]California Institute of Technology, Pasadena, CA, USA
[2]Jet Propulsion Laboratory, Pasadena, CA, USA
[3]Colorado State University, Fort Collins, CO, USA
[4]University of Wollongong, Wollongong, Australia
[5]University of Bremen, Bremen, Germany
[6]Royal Belgian Institute for Space Aeronomy, Brussels, Belgium
[7]Karlsruhe Institute of Technology (KIT), Institute of Meteorology and Climate Research (IMK-IFU), Garmisch-Partenkirchen, Germany
[8]National Institute of Water and Atmospheric Research, Auckland, New Zealand
[9]National Institute for Environmental Studies (NIES), Tsukuba, Japan
[10]Karlsruhe Institute of Technology (KIT), Institute of Meteorology and Climate Research (IMK-ASF), Karlsruhe, Germany
[11]Max Planck Institute for Biogeochemistry, Jena, Germany
[12]University of Toronto, Toronto, Canada
[13]Finnish Meteorological Institute, Sodankylä, Finland
[14]NASA Ames Research Center, Moffett Field, CA, USA
[15]Japan Aerospace Exploration Agency (JAXA), Tsukuba, Japan
[16]Los Alamos National Laboratory, Los Alamos, NM, USA
[17]AEMet, Izaña, Tenerife, Spain
[18]LERMA-IPSL, Sorbonne Universités, UPMC Univ Paris 06, CNRS, Observatoire de Paris, PSL Research University, F-75005, Paris, France
[19]Bay Area Environmental Research Institute, Petaluma, CA

Correspondence to: Debra Wunch (dwunch@gps.caltech.edu; dwunch@atmosp.physics.utoronto.ca)

Atmos. Meas. Tech. Discuss., doi:10.5194/amt-2016-227, 2016
Manuscript under review for journal Atmos. Meas. Tech.
Published: 29 August 2016

Atmospheric Measurement Techniques Discussions

Abstract. NASA's Orbiting Carbon Observatory-2 (OCO-2) has been measuring carbon dioxide column-averaged dry air mole fractions, X_{CO_2}, in the Earth's atmosphere for almost two years. In this paper, we describe the comparisons between the OCO-2 version 7Br retrievals and X_{CO_2} estimates from OCO-2's primary ground-based validation network: the Total Carbon Column Observing Network (TCCON). The OCO-2 X_{CO_2} retrievals, after bias correction, agree well globally with the TCCON for nadir, glint, and target observations, with median differences less than 0.5 ppm and RMS differences typically below 1.5 ppm. Target observations over TCCON stations correlate best with the TCCON data ($R^2 = 0.83$) on a global scale. At local scales, the target comparisons reveal residual biases likely related to surface properties and aerosol scattering. It is thus crucial to continue measurement comparisons with TCCON to monitor and evaluate the OCO-2 X_{CO_2} data quality throughout its mission.

1 Introduction

NASA's Orbiting Carbon Observatory-2 (OCO-2) is NASA's first Earth-orbiting satellite dedicated to observing atmospheric carbon dioxide (CO_2) to better understand the carbon cycle. The mission's main goal is to measure carbon dioxide with enough precision and accuracy to characterize its sources and sinks on regional scales and to quantify its seasonal and interannual variability (Crisp et al., 2008; Boland et al., 2009; Crisp, 2015). OCO-2 was successfully launched on July 2, 2014 into low-Earth orbit, and measures near infrared spectra of sunlight reflected off the Earth's surface. Carbon dioxide and oxygen (O_2) in the Earth's atmosphere absorb sunlight at well-known wavelengths in the three spectral regions observable by OCO-2, and from those absorption features, atmospheric abundances of carbon dioxide and surface pressure, and other atmospheric and surface properties (e.g., cloud and aerosol optical depth and distribution, water vapor, temperature, and surface reflectance) are obtained (O'Dell et al., 2012; Connor et al., 2008).

The main product from the retrieved abundances of carbon dioxide and surface pressure is the column-averaged dry-air mole fraction of CO_2, called X_{CO_2}, which is a useful product for carbon cycle science, as it is directly related to surface fluxes of CO_2 (Yang et al., 2007; Keppel-Aleks et al., 2011). OCO-2 measures X_{CO_2} with unprecedented precision from space (better than 1 ppm, Eldering et al., 2016) but possesses biases that the OCO-2 team have attempted to characterize and remove (Mandrake et al., 2015; O'Dell et al., 2016). To validate the OCO-2 measurements, we use the Total Carbon Column Observing Network (TCCON, Wunch et al., 2011a), a comprehensive ground-based validation network that also measures X_{CO_2}.

The OCO-2 satellite has three viewing modes: nadir mode, in which the instrument points straight down at the surface of the Earth, glint mode, in which the instrument points just off the glint spot on the surface, and target mode, in which the observatory is commanded to scan about a particular point on the ground as it passes overhead. All three modes must be independently verified using

Atmos. Meas. Tech. Discuss., doi:10.5194/amt-2016-227, 2016
Manuscript under review for journal Atmos. Meas. Tech.
Published: 29 August 2016

Atmospheric Measurement Techniques Discussions

comparisons with the ground-based TCCON data. This paper will describe the OCO-2 observation modes in §2, how the OCO-2 version 7 algorithm target-mode retrievals compare with the TCCON data in §3, and how the glint and nadir mode measurements compare with TCCON in §4.

2 OCO-2 Observation Modes

OCO-2's nadir and glint measurements are considered the nominal "science modes" of the OCO-2 measurement scheme. The nadir observations produce useful measurements only over land and near the sub-solar point over tropical oceans. The glint data are often separated into glint over land ("land glint") and glint over water ("ocean glint"), as the two modes use different surface reflectance models: Lambertian over land, and Cox-Munk over water (O'Dell et al., 2016). Retrievals are performed over a limited latitude range in glint due to concerns about biases introduced by aerosol scattering over the largest optical path lengths; see Fig. 1. The nadir mode data can provide more reliable X_{CO_2} measurements over higher latitudes over land, which is particularly important in the northern hemisphere, where the boreal forest, the driver of the CO_2 seasonal cycle, extends north of 70°N.

OCO-2 has a geographical "near-repeat" after 16 days or 233 orbits. The original measurement scheme alternated between glint and nadir observations on alternate 16-day ground track repeat cycles. This is not ideal, due to the loss of ocean measurements during nadir mode, and the loss of high latitude measurements during glint mode. Thus key components of the carbon cycle (e.g., the springtime draw down of CO_2 due to the onset of the northern hemisphere growing season) would be poorly sampled. The observing strategy was optimized to improve the coverage of the oceans and high latitude land masses on July 2, 2015 to alternate between glint and nadir modes for each subsequent orbit. The OCO-2 observation scheme was further optimized on November 12, 2015, to assign orbits that are almost entirely over ocean to be always measured in glint mode. This change was made on 72 out of the 233 orbital paths: 15 over the Atlantic and 57 over the Pacific, resulting in higher data throughput because there are now fewer nadir soundings over ocean. Crisp et al. (2016) discuss the measurement strategy in detail.

Target mode was designed to assist the OCO-2 science team in evaluating the biases in the OCO-2 X_{CO_2} product. The target locations are mostly selected to be coincident with ground validation stations, typically at TCCON sites. During a target-mode maneuver, the OCO-2 satellite rotates from its nominal science mode to point at a selected ground location. This transition takes approximately 5 minutes and rotates the spacecraft's solar panels away from the sun. The spacecraft then scans across the site or "nods" as it passes overhead to sweep across the ground several times (see Fig. 2) over a period of about 4.5 minutes: these dithered measurements comprise the "target-mode data". The spacecraft then transitions out of target mode and back into its nominal science mode over the next 5 minutes. In total, the maneuver takes about 14.5 minutes, and during this time, the spacecraft, traveling at 7.5 $\mathrm{km \cdot s^{-1}}$, has traveled over 6,500 km.

Atmos. Meas. Tech. Discuss., doi:10.5194/amt-2016-227, 2016
Manuscript under review for journal Atmos. Meas. Tech.
Published: 29 August 2016

Atmospheric Measurement Techniques Discussions

The strength of target mode measurements is that thousands of spectra are obtained in a short period of time over a small region of the world (about 0.2° longitude × 0.2° latitude for the densest measurements, Fig. 2). As long as the target location is far from large emissions sources, X_{CO_2} can be assumed constant spatially and temporally within a target measurement. However, during the maneuver, many other parameters can change, such as the atmospheric path, the path length of the measurement (the "airmass"), surface reflectivity (albedo), and topography. Any variability in the retrieved X_{CO_2} in the target mode data is considered to be an artifact, and can provide insight into biases caused by the algorithm's treatment of the parameters. With this in mind, the target locations were carefully chosen to span a wide range of latitudes, longitudes, and surface types to challenge the OCO-2 retrieval algorithm and reveal any biases caused by it.

2.1 Target Locations

There is a limited number of ground locations that can be targeted because the locations must be pre-programmed into the spacecraft software. For the first year after launch, there were 19 possible target locations. In July 2015, 8 additional targets slots became available, allowing for 27 target locations. At several times, target locations have been changed or replaced. A list of the ground target locations and dates is provided in Table 1, and a map of their locations is in Fig. 3. Individual locations can be targeted by OCO-2 only on specific OCO-2 orbit paths. Only one target location can be assigned to a given orbit path, and only if the OCO-2 ground track for that path is sufficiently close to the ground target location. Thus for each day, there are between one and seven ground target locations to choose from. The spacecraft power systems can handle up to three target-mode maneuvers per day due to the power constraints imposed by rotating the spacecraft solar panels away from the sun. We typically select only one target per day. On 40 occasions, we have targeted two locations on one day; on 3 occasions, we have targeted 3 locations on one day.

There are several TCCON stations that are located in regions with spatially varying topography or ground cover. For example, the Białystok TCCON station has a nearby forest, the Lauder TCCON station is in the midst of rolling hills, the Wollongong TCCON station is between the ocean and a sharp escarpment, the Darwin TCCON station is near the coast close to sea level, and the Edwards TCCON station is adjacent to a very bright playa, a land surface property previously identified in the Greenhouse Gases Observing Satellite (GOSAT, Kuze et al., 2009, 2016) project as challenging for X_{CO_2} retrievals (Wunch et al., 2011b). With target-mode measurements, the impact that local surface variability has on the X_{CO_2} retrievals becomes apparent.

Other TCCON stations (e.g., Park Falls, Lamont) have relatively uniform surface properties and are reasonably far from anthropogenic CO_2 sources, but the ground cover can vary from season to season. Park Falls is snow-covered in winter, dark green in summer. Lamont is green in spring and brown in winter. The Sodankylä and Eureka sites, located at high northern latitudes, challenge the OCO-2 algorithm at very high solar zenith angles and airmasses, and with snowy scenes. Izaña,

Atmos. Meas. Tech. Discuss., doi:10.5194/amt-2016-227, 2016
Manuscript under review for journal Atmos. Meas. Tech.
Published: 29 August 2016

Réunion and Ascension, all lower-latitude sites, are located on small islands remote from large land masses, but with significant topography. The Izaña TCCON station (28.3°N) is at 2.37 km altitude, whereas the Réunion (20.9°S, 0.087 km) and Ascension Island (7.9°S, 0.032 km) stations are closer to sea level.

Several TCCON target stations are near or in urban regions with varied topography and emissions sources: Pasadena is in the South Coast Air Basin of California, which contains the city of Los Angeles and is home to 17 million residents. Tsukuba is in a highly urbanized city near Tokyo (pop. ~228,000). The Paris TCCON station is located 4.5 km from the Eiffel Tower in the heart of the city (pop. ~2.24 million), and the Karlsruhe TCCON station is in a smaller, more isolated urban region (pop. ~300,000) surrounded by forest.

There are several target locations that are not TCCON stations (Fig. 3, orange stars), and although data from those targets will not be analysed in this paper, the data will help assess bias. Railroad Valley is a heavily instrumented radiometric calibration site (Kuze et al., 2011); Shanghai, São Paulo and Mexico City are geographically well-constrained urban regions with significant CO_2 emissions; Rosemount and Litchfield have instrumentation that will help verify the OCO-2 solar induced fluorescence observations; Boulder has frequent AirCore CO_2 profile measurements (Karion et al., 2010); Fairbanks is a future TCCON station. The Libya location has very specific and consistent surface properties and observations there will improve the radiometric calibration of OCO-2.

2.2 Target Selection

Target locations are selected a day or two in advance, based on the weather forecast, the operational status of the TCCON station (if the target is a TCCON station), the importance of the projected data loss in nadir or glint mode from performing the target-mode operation, and the historical statistics of successful target-mode measurements over that site. The projected data loss depends primarily on whether the nominal mode for that orbit was nadir over land, nadir over ocean, glint over land, or glint over ocean. If the nominal mode is nadir over ocean, little data loss occurs, as nadir measurements over ocean are usually too dark in the near infrared for successful retrievals: in this case, the target is almost always selected given a reasonable weather forecast. This has mostly been the case for Réunion Island, which has been targeted regularly from OCO-2 nadir orbits. For the other three cases, there will be some loss of regular science data to accommodate a target-mode operation. In these cases, the historical statistics of acquiring good target-mode data and weather forecasts are weighted more heavily before enabling the target. Often, if the weather forecast is not ideal, no target-mode measurements will be selected.

As of April 30, 2016, 227 targets have been selected, 195 of them over TCCON stations (Fig. 4). Of the 195 targets of TCCON stations, about 90% were "successful", in that both OCO-2 data and TCCON data were recorded. This 10% loss was largely due to poor weather forecasts, resulting in completely overcast skies, during which the TCCON station was unable to record any data.

Atmos. Meas. Tech. Discuss., doi:10.5194/amt-2016-227, 2016
Manuscript under review for journal Atmos. Meas. Tech.
Published: 29 August 2016

Atmospheric Measurement Techniques Discussions

There were two instances of unforeseen mechanical failures at TCCON stations. Of the 195 targets recorded, about 55% were clear enough to obtain sufficient high-quality (low warn level) OCO-2 data to compare with TCCON data.

3 Target Mode Comparisons to TCCON and Residual Bias Assessment

All current space-based X_{CO_2} measurements have systematic biases caused by uncertainties in the spectroscopy, by limitations in the information content of the measurements and uncertainties or oversimplifications in the optical properties of the atmosphere and surface, and by uncertainties in the instrument characterization and calibration (e.g., Crisp et al., 2016; Wunch et al., 2011a; Guerlet et al., 2013; Schneising et al., 2012). Considerable effort is dedicated to creating robust "bias corrections". There are three key types of biases considered here, and the bias correction addresses them all: the first is any constant scaling factor from the World Meteorological Organization (WMO) trace-gas standard scale (a "constant" bias), the second is spurious correlations of the retrieved X_{CO_2} with other retrieval parameters such as the surface pressure retrieval error, signal level, airmass, surface albedo (a "parameter-dependent" bias), and the third is any footprint-dependent biases. Footprint-dependent biases are corrected with calibration observations compiled using a special subset of OCO-2 data collected while the spectrometer slit is oriented parallel to the ground track and the eight OCO-2 footprints are geographically coincident (Mandrake et al., 2015). The parameter-dependent biases must be removed before the constant scaling factor can be established, as the parameter-dependent bias correction can impact the magnitude of the constant scaling factor. The procedure by which the OCO-2 data have been bias-corrected is documented in detail by Mandrake et al. (2015) and O'Dell et al. (2016) and is briefly described here. The parameter-dependent bias correction uses a genetic algorithm to determine which retrieval parameters account for the largest fraction of the spurious variability found in the estimated X_{CO_2} on large spatial scales. The algorithm uses several subsets of the OCO-2 data for this task: a "southern hemisphere approximation" which exploits the low spatial and temporal variability of X_{CO_2} in the the southern hemisphere south of 25°S (e.g., Wunch et al., 2011b); a "small area analysis" which exploits the low spatial variability of X_{CO_2} within small regions (0.89° latitude on a single orbit track) and can be applied at all latitudes; and data near coastlines wherein differences in X_{CO_2} between land and ocean can be clearly diagnosed. A multivariate regression is performed between spurious X_{CO_2} variability and the parameters. The resulting slopes of the regressions allow us to then subtract the predicted bias from the X_{CO_2} values. In the results that follow, the parameter-dependent biases in the OCO-2 target-mode data have been removed following Mandrake et al. (2015), allowing us to determine the constant scaling factor.

Placing the OCO-2 data on the World Meteorological Organization's (WMO) trace-gas standard scale is crucial to obtaining flux inversions consistent with the state-of-the-art inversions of surface

Atmos. Meas. Tech. Discuss., doi:10.5194/amt-2016-227, 2016
Manuscript under review for journal Atmos. Meas. Tech.
Published: 29 August 2016

Atmospheric Measurement Techniques Discussions

in situ CO_2 data, which are carefully calibrated to the WMO scale (Zhao and Tans, 2006). To achieve this, we compare the OCO-2 target mode data with the latest version of the TCCON data (GGG2014, Wunch et al., 2015), which have been tied to the WMO trace-gas standard scale through comparisons with in situ CO_2 profiles from aircraft (Wofsy, 2011; Pan et al., 2010; Singh et al., 2006) and AirCore (Karion et al., 2010), following the methods described by Wunch et al. (2010). We consider TCCON data to be coincident with the OCO-2 target-mode measurements when they have been recorded within ± 30 minutes of the time at which the spacecraft is closest to nadir during the maneuver. If there are fewer than 5 TCCON data points recorded within that time, the window is extended to ± 120 minutes, but this is required in only 14% of cases. We use the full OCO-2 version 7B retrospective data (i.e., 7Br), available from GES-DISC (2016, http://disc.sci.gsfc.nasa.gov/OCO-2), and manually apply the filters listed in Table 2. These filters are consistent with the "warn level 15" scheme described by Mandrake et al. (2015), except that the filter on the surface pressure difference from the prior in the A-band pre-processor is loosened, and we have added an additional outlier filter.

Figure 5 shows the OCO-2 X_{CO_2} target-mode median data comparisons with coincident TCCON data. The best fit lines were computed using a method that accounts for uncertainties in the dependent and independent variables as described by York et al. (2004). Panel (a) shows the results prior to applying the parameter-dependent bias correction and has a correlation coefficient of $R^2 = 0.75$. Panel (b) shows the relationship after the correction has been applied and an improved correlation coefficient ($R^2 = 0.83$). The improvement indicates that the parameter-dependent bias correction is effective at removing spurious variability in the OCO-2 data. The slope in panel (b), which has a y-intercept that is forced through 0, is used to derive the constant scaling factor between TCCON and OCO-2 target observations ($m = 0.9975 \pm 0.04$, which represents ~1 ppm) for the time period spanning September 8, 2014 through April 30, 2016. The time-dependence of the difference between the OCO-2 target-mode data and the coincident TCCON data (ΔX_{CO_2}), after the constant bias is removed, is plotted in Fig. 6. The algorithm, calibration and instrument cause no apparent time-dependent drift in ΔX_{CO_2} nor their errors. Thus, the bias correction is successful at reducing both the parameter-dependent and constant global biases.

However, the target mode measurements are sensitive enough to point to some residual biases that are currently under investigation by the OCO-2 algorithm, calibration and validation teams. These residual biases are more geographically localized in nature, and as such might not be expected to be captured by the standard bias correction, which is designed to minimize globally-relevant biases. The residual biases seem to fall into two classes: biases in high southern latitude ocean glint data (§3.1), and biases caused by the surface properties at a target location (§3.2).

3.1 Southern hemisphere winter glint measurements over water

In the southern hemisphere winter, there is a significant high bias in the retrieved X_{CO_2} from the OCO-2 ocean glint data. There were three target-mode measurements recorded in the southern hemi-

Atmos. Meas. Tech. Discuss., doi:10.5194/amt-2016-227, 2016
Manuscript under review for journal Atmos. Meas. Tech.
Published: 29 August 2016

Atmospheric Measurement Techniques Discussions

sphere during that time: two points over Wollongong, and a third point over Réunion recorded during late July/early August 2015 (Fig. 6). Figure 7 illustrates this problem by showing the divergence of the latitude gradients of the OCO-2 X_{CO_2} in all viewing modes and the TCCON X_{CO_2} during August 2015 and the agreement in October 2015. Appendix Fig. A1 panels (r) and (s) also show this problem as a function of time. This bias does not impact the overall one-to-one line within the uncertainty but does impact the latitudinal gradients (and hence fluxes) inferred by the OCO-2 data. While the cause of the bias in the southern winter is currently unclear, there is a working hypothesis related to the OCO-2 algorithm's misrepresentation of stratospheric aerosols, exacerbated by the eruption of Mount Calbuco in Chile on April 22, 2015 (Romero et al., 2016). This is described in detail in O'Dell et al. (2016).

3.2 Surface Properties

Site-dependent differences from the one-to-one plot, shown in Fig. 8, reveal significant location-dependent biases. Any differences with magnitudes less than 0.3 ppm could be attributable to TCCON station site-to-site biases (Wunch et al., 2010), so we focus on the biases that are significantly larger and thus attributable to the OCO-2 data. Two clear examples of site-dependent biases are at Edwards, with a mean low bias of ~1.3 ppm, and Wollongong, with a mean high bias of ~0.9 ppm. The spatial dependence of the target-mode measurements reveal that small-scale variability in surface properties (e.g., albedo, altitude, surface roughness) can cause significant and spurious variability in the X_{CO_2}.

The Edwards TCCON station is situated in the bright California high desert on the edge of a very bright playa with little topographic change. On some, but not all targets over Edwards, the X_{CO_2} appears dependent on surface brightness (Fig. 9). All mean target-mode measurements of X_{CO_2} at Edwards are biased lower than the TCCON measurements. Conversely, the Wollongong station, which is situated near the East coast of Australia, is a very dark surface in the visible, and lies between the Tasman Sea to the East and the Illawarra Escarpment to the West (Fig. 10). The OCO-2 retrievals of X_{CO_2} are systematically higher than the TCCON measurements for all target-mode measurements, and are particularly high (up to 5 ppm) in July and August (Fig. 11), due to the problem discussed above in §3.1. OCO-2 data over Białystok, located in a dark, forested region, also has a persistent high bias (on the order of 1.3 ppm) compared with TCCON.

Even at sites which do not appear to have a significant bias with respect to TCCON can show spurious spatially-correlated errors. The Lauder TCCON station is situated in a valley between rolling hills (Fig. 12). The surface altitude is spatially well-correlated with changes in X_{CO_2} during each target-mode maneuver.

In the standard OCO-2 retrieval algorithm, land surfaces are assumed to have a Lambertian bidirectional reflectance distribution function (BRDF, O'Dell et al., 2012). A more complex BRDF that can better model changes in surface topography and vegetation is currently undergoing testing

Atmos. Meas. Tech. Discuss., doi:10.5194/amt-2016-227, 2016
Manuscript under review for journal Atmos. Meas. Tech.
Published: 29 August 2016

Atmospheric Measurement Techniques Discussions

and shows promise for reducing the problems addressed above (Natraj et al., 2015). An improved treatment of the surface properties will be included in the next version of the OCO-2 data.

4 Nadir and Glint Mode Comparisons to TCCON

In this section, we evaluate the bias-corrected OCO-2 glint and nadir modes against ground-based TCCON data to reveal mode-dependent biases that were not eliminated using the standard version 7 bias correction. We use the version 7B retrospective OCO-2 "lite" files here, which have had the footprint-dependent, parameter-dependent, and constant scaling biases removed, and we limit ourselves to data for which the "warn level" is less than or equal to 11 (Mandrake et al., 2013, 2015), and the "outcome_flag" is zero. These data are available from the CO_2 Virtual Science Data Environment (JPL-Caltech, 2016, http://co2.jpl.nasa.gov) and from GES-DISC (2016). For these comparisons, we choose the following coincidence criteria: a box centred around the TCCON station that spans 5° in latitude and 10° in longitude on the same day as a TCCON measurement, with the exceptions mentioned below. In the southern hemisphere south of 25°S, we use a larger box spanning 20° in latitude and 120° in longitude because the geographical variance in X_{CO_2} in the southern hemisphere is low (e.g., Wunch et al., 2011b). The Edwards and Pasadena boxes are constructed differently because they are geographically very close to each other, but the Pasadena site is within the polluted, mountain-contained South Coast Air Basin, and Edwards is in the clean desert north of the mountains. Thus, we limit the Edwards latitudes to north of Edwards, but allow the longitudes to span 5° further west over the Pacific Ocean. The Pasadena coincidence box is constrained to the South Coast Air Basin, which significantly limits the number of coincident points (see Appendix Figs. A1(a-t)). The median of the measurements within the coincidence box on the same day as the TCCON measurement is compared with the TCCON daily median. The more complicated dynamical coincidence criteria used to increase the number of coincident measurements between TCCON and GOSAT in Wunch et al. (2011b) and Nguyen et al. (2014) are not required for OCO-2, due to OCO-2's much higher data density.

The overall comparisons between the OCO-2 data and TCCON data are reported in Tables 3 and 4, and shown in Figs. 13–15 for data from land glint mode, ocean glint mode, and nadir mode. The biases between OCO-2 and TCCON are all less than 0.5 ppm, and the RMS of the difference is less than about 1.5 ppm. The nadir mode data show the best correlation of the three science modes ($R^2 = 0.75$), followed by land glint ($R^2 = 0.72$), and finally ocean glint ($R^2 = 0.50$). The low correlation coefficient in the ocean glint data is partially driven by the high anomalies in the southern hemisphere winter, most obviously in the data over Wollongong (Fig. 7), and also because a high proportion of ocean glint data are in the southern hemisphere, where X_{CO_2} variability is lower. If the southern hemisphere winter data (June–September) are excluded from the ocean glint correlations, the R^2 improves to 0.71. The slopes of all three curves are significantly different from 1.0. The

Atmos. Meas. Tech. Discuss., doi:10.5194/amt-2016-227, 2016
Manuscript under review for journal Atmos. Meas. Tech.
Published: 29 August 2016

agreement between the science-mode OCO-2 data and TCCON is poorer than that for the target-mode measurements. Halving the spatial coincidence criteria over each site does not significantly improve the correlation coefficients ($R^2 = 0.78, 0.73, 0.58, 0.77$ for nadir, land glint, ocean glint, and ocean glint excluding the southern hemisphere winter, respectively) and the slopes increase, but well within the uncertainties. This suggests that it is not solely our definition of the coincidence criteria that causes the low correlation coefficients, and that perhaps the surface properties within the coincidence boxes contain sufficient variability to degrade the comparisons. This highlights the importance of the target-mode data for assessing local, site-to-site, and overall bias.

5 Conclusions

The OCO-2 X_{CO_2} estimates generally compare well with coincident TCCON data at global scales, with mean biases less than 0.5 ppm and RMS differences less than about 1.5 ppm. The best comparisons are with the target-mode data, which is expected because the target mode measurement scheme was designed for this purpose. The target-mode data are also particularly well-suited to tying the OCO-2 data to the WMO trace gas scale through comparisons with the TCCON data, because they best represent coincident measurements under invariant atmospheric conditions. While the bias correction clearly improves the relationship between TCCON and OCO-2 globally, smaller-scale biases, typically < 2 ppm, remain. Examples of these biases include spurious local X_{CO_2} variability correlated with topography and surface brightness, and ocean glint measurements at southern latitudes during the southern hemisphere winter. Remedying these residual biases is the current focus of the OCO-2 algorithm development and validation teams and we anticipate that the next version of the OCO-2 data will represent a significant improvement. It is imperative to continue measurement comparisons with TCCON in all three modes (target, glint and nadir) to monitor and evaluate the OCO-2 data quality throughout its entire mission.

6 Data Availability

Unfiltered, uncorrected OCO-2 data are available from the Goddard Data Center (GES-DISC, 2016). The filtered and bias-corrected data are contained in "lite" files, which are available from JPL's CO_2 portal (JPL-Caltech, 2016). TCCON data are available from the TCCON data archive, hosted by CDIAC: http://tccon.ornl.gov. Each TCCON dataset used in this paper is cited independently in Table 1 or in the captions of Fig. A1.

Appendix A: Site Plots

The ocean glint, land glint and nadir mode plots for each TCCON station are shown in Fig. A1. In each plot, there are four panels. The top left panel shows the time series of the TCCON daily median

Atmos. Meas. Tech. Discuss., doi:10.5194/amt-2016-227, 2016
Manuscript under review for journal Atmos. Meas. Tech.
Published: 29 August 2016

Atmospheric Measurement Techniques Discussions

data (black circles) and the OCO-2 data (triangles coloured differently for each mode). The bottom left panel shows the difference between OCO-2 and TCCON measurements (OCO-2 – TCCON). The top right panel shows the correlations between the TCCON data and the OCO-2 data. The bottom right panel shows the coincidence area for the OCO-2 measurements.

Appendix B: Author contributions

DW wrote the manuscript and produced the main analysis and results with significant input from GO, CV, and POW. DW, GO, BF, BN, CMR, CO, AE, LM, CV, MRG, DC, and POW contributed to the experiment design and analysis of data. DWTG, NMD, VAV, JN, TW, CP, MdM, MKS, RS, MR, DP, JR, IM, OU, FH, TB, MK, DGF, SGA, KS, JM, RK, PH, LI, JP, PH, SK, MD, HAP, ES, OEGR, YT, PJ, provided TCCON data. All authors read and provided comments on the manuscript.

Acknowledgements. Part of this work was performed at the Jet Propulsion Laboratory, California Institute of Technology, under contract with NASA. Operation of the Ascension Island site was funded by the Max Planck Society. The Bremen, Białystok, and Orléans TCCON sites are funded by the EU projects InGOS and ICOS-INWIRE, and by the Senate of Bremen. The Darwin and Wollongong TCCON sites are funded by NASA grants NAG512247 and NNG05GD07G, and Australian Research Council grants DP140101552, DP110103118, DP0879468, LE0668470, and LP0562346. We are grateful to the DOE ARM program for technical support at the Darwin TCCON site. ND was supported by an Australian Research Council fellowship, DE140100178. The TCCON site at Île de la Réunion is operated by the Royal Belgian Institute for Space Aeronomy with financial support in 2014, 2015 and 2016 under the EU project ICOS-Inwire and the ministerial decree for ICOS (FR/35/IC2) and local activities supported by LACy/UMR8105 - Université de La Réunion. TCCON is funded by NASA grants NNX14AI60G, NNX11AG01G, NAG5-12247, NNG05-GD07G, and NASA's Orbiting Carbon Observatory Program. We are grateful to the DOE ARM program for technical support in Lamont and Jeff Ayers for technical support in Park Falls. From 2004 to 2011 the Lauder TCCON programme was funded by the New Zealand Foundation of Research Science and Technology contracts CO1X0204, CO1X0703 and CO1X0406. Since 2011 the programme has been funded by NIWA's Atmosphere Research Programme 3 (2011/13 Statement of Corporate Intent). The TCCON measurements at Eureka are made by the Canadian Network for the Detection of Atmospheric Change (CANDAC), led by James R. Drummond, and in part by the Canadian Arctic ACE Validation Campaigns, led by Kaley A. Walker. They are supported by the Atlantic Innovation Fund/Nova Scotia Research Innovation Trust, Canada Foundation for Innovation, Canadian Foundation for Climate and Atmospheric Sciences, Canadian Space Agency, Environment Canada, Government of Canada International Polar Year funding, Natural Sciences and Engineering Research Council, Northern Scientific Training Program, Ontario Innovation Trust, Ontario Research Fund and Polar Continental Shelf Program. We thank PEARL site manager Pierre Fogal, the staff at the Eureka weather station, and the CANDAC operators for the logistical and on-site support provided at Eureka. MKD thanks DOE OBER's TES and NGEE-Tropics program for funding and ARM for logistical support of the TCCON deployment during the GoAmazon campaign.

Atmos. Meas. Tech. Discuss., doi:10.5194/amt-2016-227, 2016
Manuscript under review for journal Atmos. Meas. Tech.
Published: 29 August 2016

Atmospheric Measurement Techniques Discussions

References

Blumenstock, T., Hase, F., Schneider, M., Garcia, O., and Sepulveda, E.: TCCON data from Izana, Tenerife, Spain, Release GGG2014R0, TCCON data archive, hosted by the Carbon Dioxide Information Analysis Center, Oak Ridge National Laboratory, Oak Ridge, Tennessee, U.S.A., http://dx.doi.org/10.14291/tccon.ggg2014.izana01.R0/1149295, doi:10.14291/tccon.ggg2014.izana01.R0/1149295, 2014.

Boland, S., Brown, L. R., Burrows, J. P., Ciais, P., Connor, B. J., Crisp, D., Denning, A. S., Doney, S. C., Engelen, R., Fung, I. Y., Griffith, P., Jacob, D. J., Johnson, B., Martin-Torres, J., Michalak, A. M., Miller, C. E., Polonsky, I., Potter, C., Randerson, J. T., Rayner, P. J., Salawitch, R. J., Santee, M., Tans, P. P., Wennberg, P. O., Wunch, D., Wofsy, S. C., and Yung, Y. L.: The Need for Atmospheric Carbon Dioxide Measurements from Space : Contributions from a Rapid Reflight of the Orbiting Carbon Observatory, Tech. rep., 2009.

Connor, B. J., Boesch, H., Toon, G. C., Sen, B., Miller, C. E., and Crisp, D.: Orbiting Carbon Observatory: Inverse method and prospective error analysis, Journal of Geophysical Research, 113, 1–14, doi:10.1029/2006JD008336, http://www.agu.org/pubs/crossref/2008/2006JD008336.shtml, 2008.

Crisp, D.: Measuring atmospheric carbon dioxide from space with the Orbiting Carbon Observatory-2 (OCO-2), in: SPIE, vol. 9607, pp. 960 702–1, doi:10.1117/12.2187291, http://proceedings.spiedigitallibrary.org/proceeding.aspx?doi=10.1117/12.2187291, 2015.

Crisp, D., Miller, C. E., and DeCola, P. L.: NASA Orbiting Carbon Observatory: measuring the column averaged carbon dioxide mole fraction from space, Journal Of Applied Remote Sensing, 2, 23 508, doi:10.1117/1.2898457, http://scitation.aip.org/getabs/servlet/GetabsServlet?prog=normal{&}id=JARSC400000200000102350800000 1{&}idtype=cvips{&}gifs=yes{\T1\textbackslash}npapers2://publication/doi/10.1117/1.2898457, 2008.

Crisp, D., Chapsky, L., Eldering, A., Fisher, B., Frankenberg, C., Gunson, M. R., Lee, R., Osterman, G. B., Oyafuso, F., O'Dell, C. W., Pollock, R., Taylor, T. E., Wennberg, P. O., and Wunch, D.: The On-Orbit Performance of the Orbiting Carbon Observatory (OCO-2), Atmos. Meas. Tech., in prep., 2016.

De Maziere, M., Sha, M. K., Desmet, F., Hermans, C., Scolas, F., Kumps, N., Metzger, J.-M., Duflot, V., and Cammas, J.-P.: TCCON data from Reunion Island (La Reunion), France, Release GGG2014R0, TCCON data archive, hosted by the Carbon Dioxide Information Analysis Center, Oak Ridge National Laboratory, Oak Ridge, Tennessee, U.S.A., http://dx.doi.org/10.14291/tccon.ggg2014.reunion01.R0/1149288, doi:10.14291/tccon.ggg2014.reunion01.R0/1149288, 2014.

Deutscher, N. M., Notholt, J., Messerschmidt, J., Weinzierl, C., Warneke, T., Petri, C., Grupe, P., and Katrynski, K.: TCCON data from Bialystok, Poland, Release GGG2014R1, TCCON data archive, hosted by the Carbon Dioxide Information Analysis Center, Oak Ridge National Laboratory, Oak Ridge, Tennessee, U.S.A., http://dx.doi.org/10.14291/tccon.ggg2014.bialystok01.R1/1183984, doi:10.14291/tccon.ggg2014.bialystok01.R1/1183984, 2014.

Dubey, M., Henderson, B., Green, D., Butterfield, Z., Keppel-Aleks, G., Allen, N., Blavier, J.-F., Roehl, C., Wunch, D., and Lindenmaier, R.: TCCON data from Manaus, Brazil, Release GGG2014R0, TCCON data archive, hosted by the Carbon Dioxide Information Analysis Center, Oak Ridge National Laboratory, Oak Ridge, Tennessee, U.S.A., http://dx.doi.org/10.14291/tccon.ggg2014.manaus01.R0/1149274, doi:10.14291/tccon.ggg2014.manaus01.R0/1149274, 2014.

Atmos. Meas. Tech. Discuss., doi:10.5194/amt-2016-227, 2016
Manuscript under review for journal Atmos. Meas. Tech.
Published: 29 August 2016

Eldering, A., O'Dell, C. W., Wennberg, P. O., Crisp, D., Gunson, M., Viatte, C., Avis, C., Braverman, A., Bruegge, C., Castano, R., Chang, A., Chapsky, L., C. Cheng, B. C., Dang, L., Doran, G., Fisher, B., Frankenberg, C., Fu, D., Granat, R., Hobbs, J., Lee, R., Mandrake, L., McDuffie, J., Myers, V., Natraj, V., O'Brien, D., Osterman, G., Oyafuso, F., Payne, V., Pollock, H., Polonsky, I., Roehl, C., Rosenberg, R., Smyth, M., Tang, V., Taylor, T., To, C., Wunch, D., and Yoshimizu, J.: The Orbiting Carbon Observatory-2: First Year Status and Results, Atmos. Meas. Tech., 2016.

Feist, D. G., Arnold, S. G., John, N., and Geibel, M. C.: TCCON data from Ascension Island, Saint Helena, Ascension and Tristan da Cunha, Release GGG2014R0, TCCON data archive, hosted by the Carbon Dioxide Information Analysis Center, Oak Ridge National Laboratory, Oak Ridge, Tennessee, U.S.A., http://dx.doi.org/10.14291/tccon.ggg2014.ascension01.R0/1149285, doi:10.14291/tccon.ggg2014.ascension01.R0/1149285, 2014.

GES-DISC: Goddard Earth Sciences Data and Information Services Center OCO-2 Data Holdings, http://disc.sci.gsfc.nasa.gov/OCO-2, 2016.

Griffith, D. W. T., Deutscher, N. M., Velazco, V. A., Wennberg, P. O., Yavin, Y., Aleks, G. K., Washenfelder, R., Toon, G. C., Blavier, J.-F., Murphy, C., Jones, N., Kettlewell, G., Connor, B. J., Macatangay, R., Roehl, C., Ryczek, M., Glowacki, J., Culgan, T., and Bryant, G.: TCCON data from Darwin, Australia, Release GGG2014R0, TCCON data archive, hosted by the Carbon Dioxide Information Analysis Center, Oak Ridge National Laboratory, Oak Ridge, Tennessee, U.S.A., http://dx.doi.org/10.14291/tccon.ggg2014.darwin01.R0/1149290, doi:10.14291/tccon.ggg2014.darwin01.R0/1149290, 2014a.

Griffith, D. W. T., Velazco, V. A., Deutscher, N. M., Murphy, C., Jones, N., Wilson, S., Macatangay, R., Kettlewell, G., Buchholz, R. R., and Riggenbach, M.: TCCON data from Wollongong, Australia, Release GGG2014R0, TCCON data archive, hosted by the Carbon Dioxide Information Analysis Center, Oak Ridge National Laboratory, Oak Ridge, Tennessee, U.S.A., http://dx.doi.org/10.14291/tccon.ggg2014.wollongong01.R0/1149291, doi:10.14291/tccon.ggg2014.wollongong01.R0/1149291, 2014b.

Guerlet, S., Butz, A., Schepers, D., Basu, S., Hasekamp, O. P., Kuze, A., Yokota, T., Blavier, J.-F. L., Deutscher, N. M., Griffith, D. W. T., Hase, F., Kyro, E., Morino, I., Sherlock, V., Sussmann, R., Galli, A., and Aben, I.: Impact of aerosol and thin cirrus on retrieving and validating XCO 2 from GOSAT shortwave infrared measurements, Journal of Geophysical Research: Atmospheres, 118, 4887–4905, doi:10.1002/jgrd.50332, http://doi.wiley.com/10.1002/jgrd.50332, 2013.

Hase, F., Blumenstock, T., Dohe, S., Gross, J., and Kiel, M.: TCCON data from Karlsruhe, Germany, Release GGG2014R1, TCCON data archive, hosted by the Carbon Dioxide Information Analysis Center, Oak Ridge National Laboratory, Oak Ridge, Tennessee, U.S.A., http://dx.doi.org/10.14291/tccon.ggg2014.karlsruhe01.R1/1182416, doi:10.14291/tccon.ggg2014.karlsruhe01.R1/1182416, 2014.

Iraci, L., Podolske, J., Hillyard, P., Roehl, C., Wennberg, P. O., Blavier, J.-F., Landeros, J., Allen, N., Wunch, D., Zavaleta, J., Quigley, E., Osterman, G., Albertson, R., Dunwoody, K., and Boyden, H.: TCCON data from Armstrong Flight Research Center, Edwards, CA, USA, Release GGG2014R0, TCCON data archive, hosted by the Carbon Dioxide Information Analysis Center, Oak Ridge National Labo-

ratory, Oak Ridge, Tennessee, U.S.A., http://dx.doi.org/10.14291/tccon.ggg2014.edwards01.R0/1149289, doi:10.14291/tccon.ggg2014.edwards01.R0/1149289, 2014.

JPL-Caltech: CO2 Virtual Science Data Environment, http://co2.jpl.nasa.gov, 2016.

Karion, A., Sweeney, C., Tans, P. P., and Newberger, T.: AirCore: An Innovative Atmospheric Sampling System, Journal of Atmospheric and Oceanic Technology, 27, 1839–1853, doi:10.1175/2010JTECHA1448.1, http://journals.ametsoc.org/doi/abs/10.1175/2010JTECHA1448.1, 2010.

Kawakami, S., Ohyama, H., Arai, K., Okumura, H., Taura, C., Fukamachi, T., and Sakashita, M.: TCCON data from Saga, Japan, Release GGG2014R0, TCCON data archive, hosted by the Carbon Dioxide Information Analysis Center, Oak Ridge National Laboratory, Oak Ridge, Tennessee, U.S.A., http://dx.doi.org/10.14291/tccon.ggg2014.saga01.R0/1149283, doi:10.14291/tccon.ggg2014.saga01.R0/1149283, 2014.

Keppel-Aleks, G., Wennberg, P. O., and Schneider, T.: Sources of variations in total column carbon dioxide, Atmospheric Chemistry and Physics, 11, 3581–3593, doi:10.5194/acp-11-3581-2011, http://www.atmos-chem-phys.net/11/3581/2011/, 2011.

Kivi, R., Heikkinen, P., and Kyro, E.: TCCON data from Sodankyla, Finland, Release GGG2014R0, TCCON data archive, hosted by the Carbon Dioxide Information Analysis Center, Oak Ridge National Laboratory, Oak Ridge, Tennessee, U.S.A., http://dx.doi.org/10.14291/tccon.ggg2014.sodankyla01.R0/1149280, doi:10.14291/tccon.ggg2014.sodankyla01.R0/1149280, 2014.

Kuze, A., Suto, H., Nakajima, M., and Hamazaki, T.: Thermal and near infrared sensor for carbon observation Fourier-transform spectrometer on the Greenhouse Gases Observing Satellite for greenhouse gases monitoring., Applied optics, 48, 6716–6733, doi:10.1364/AO.48.006716, http://ao.osa.org/abstract.cfm?URI=ao-48-35-6716{\T1\textbackslash}nhttp://www.opticsinfobase.org/DirectPDFAccess/68E1C66A-0570-929E-8DC1BEA9D7180E52{_}190794/ao-48-35-6716.pdf?da=1{&}id=190794{&}seq=0{&}mobile=no, 2009.

Kuze, A., O'Brien, D. M., Taylor, T. E., Day, J. O., O'Dell, C. W., Kataoka, F., Yoshida, M., Mitomi, Y., Bruegge, C. J., Pollock, H., Basilio, R., Helmlinger, M., Matsunaga, T., Kawakami, S., Shiomi, K., Urabe, T., and Suto, H.: Vicarious Calibration of the GOSAT Sensors Using the Railroad Valley Desert Playa, IEEE Transactions on Geoscience and Remote Sensing, 49, 1781–1795, doi:10.1109/TGRS.2010.2089527, http://ieeexplore.ieee.org/xpls/abs{_}all.jsp?arnumber=5659476http://ieeexplore.ieee.org/lpdocs/epic03/wrapper.htm?arnumber=5659476, 2011.

Kuze, A., Suto, H., Shiomi, K., Kawakami, S., Tanaka, M., Ueda, Y., Deguchi, A., Yoshida, J., Yamamoto, Y., Kataoka, F., Taylor, T. E., and Buijs, H.: Update on GOSAT TANSO-FTS performance, operations, and data products after more than six years in space, Atmospheric Measurement Techniques Discussions, 2014, 1–38, doi:10.5194/amt-2015-333, http://www.atmos-meas-tech-discuss.net/amt-2015-333/, 2016.

Mandrake, L., Frankenberg, C., O'Dell, C. W., Osterman, G., Wennberg, P. O., and Wunch, D.: Semi-autonomous sounding selection for OCO-2, Atmospheric Measurement Techniques, 6, 2851–2864, doi:10.5194/amt-6-2851-2013, http://www.atmos-meas-tech.net/6/2851/2013/, 2013.

Mandrake, L., O'Dell, C. W., Wunch, D., Wennberg, P. O., Fisher, B., Osterman, G. B., and Eldering, A.: Orbiting Carbon Observatory-2 (OCO-2) Warn Level, Bias Correction, and Lite File Product Description, Tech. rep., Jet Propulsion Laboratory, California Insti-

tute of Technology, Pasasdena, http://disc.sci.gsfc.nasa.gov/OCO-2/documentation/oco-2-v7/OCO2{_}XCO2{_}Lite{_}Files{_}and{_}Bias{_}Correction{_}0915{_}sm.pdf, 2015.

McGill, R., Tukey, J. W., and Larsen, W. a.: Variations of Box Plots, The American Statistician, 32, 12–16, doi:10.2307/2683468, 1978.

Morino, I., Matsuzaki, T., and Shishime, A.: TCCON data from Tsukuba, Ibaraki, Japan, 125HR, Release GGG2014R1, TCCON data archive, hosted by the Carbon Dioxide Information Analysis Center, Oak Ridge National Laboratory, Oak Ridge, Tennessee, U.S.A., http://dx.doi.org/10.14291/tccon.ggg2014.tsukuba02.R1/1241486, doi:10.14291/tccon.ggg2014.tsukuba02.R1/1241486, 2014a.

Morino, I., Yokozeki, N., Matzuzaki, T., and Shishime, A.: TCCON data from Rikubetsu, Hokkaido, Japan, Release GGG2014R1, TCCON data archive, hosted by the Carbon Dioxide Information Analysis Center, Oak Ridge National Laboratory, Oak Ridge, Tennessee, U.S.A., http://dx.doi.org/10.14291/tccon.ggg2014.rikubetsu01.R1/1242265, doi:10.14291/tccon.ggg2014.rikubetsu01.R1/1242265, 2014b.

Natraj, V., McDuffie, J. L., O'Dell, C. W., Eldering, A., Fu, D., and Wunch, D.: Assessing Surface BRDF-related Biases Using Target Mode Retrievals from the Orbiting Carbon Observatory-2 (OCO-2), American Geophysical Union Fall Meeting, 2015.

Nguyen, H., Osterman, G., Wunch, D., O'Dell, C. W., Mandrake, L., Wennberg, P. O., Fisher, B., and Castano, R.: A method for colocating satellite XCO2 data to ground-based data and its application to ACOS-GOSAT and TCCON, Atmospheric Measurement Techniques, 7, 2631–2644, doi:10.5194/amt-7-2631-2014, http://www.atmos-meas-tech.net/7/2631/2014/, 2014.

Notholt, J., Petri, C., Warneke, T., Deutscher, N. M., Buschmann, M., Weinzierl, C., Macatangay, R., and Grupe, P.: TCCON data from Bremen, Germany, Release GGG2014R0, TCCON data archive, hosted by the Carbon Dioxide Information Analysis Center, Oak Ridge National Laboratory, Oak Ridge, Tennessee, U.S.A., http://dx.doi.org/10.14291/tccon.ggg2014.bremen01.R0/1149275, doi:10.14291/tccon.ggg2014.bremen01.R0/1149275, 2014.

O'Dell, C. W., Connor, B. J., Bösch, H., O'Brien, D. M., Frankenberg, C., Castano, R., Christi, M., Eldering, D., Fisher, B., Gunson, M., McDuffie, J., Miller, C. E., Natraj, V., Oyafuso, F. A., Polonsky, I., Smyth, M., Taylor, T. E., Toon, G. C., Wennberg, P. O., and Wunch, D.: The ACOS CO2 retrieval algorithm – Part 1: Description and validation against synthetic observations, Atmospheric Measurement Techniques, 5, 99–121, doi:10.5194/amt-5-99-2012, http://www.atmos-meas-tech.net/5/99/2012/, 2012.

O'Dell, C. W., Wennberg, P. O., Eldering, A., Crisp, D., Gunson, M. R., and Fisher, B.: The OCO-2 Retrieval Algorithm, Atmospheric Measurement Techniques, in prep, 2016.

Pan, L. L., Bowman, K. P., Atlas, E. L., Wofsy, S. C., Zhang, F., Bresch, J. F., Ridley, B. A., Pittman, J. V., Homeyer, C. R., Romashkin, P. A., and Cooper, W. A.: The Stratosphere–Troposphere Analyses of Regional Transport 2008 Experiment, Bulletin of the American Meteorological Society, 91, 327–342, doi:10.1175/2009BAMS2865.1, http://journals.ametsoc.org/doi/abs/10.1175/2009BAMS2865.1, 2010.

Romero, J. E., Morgavi, D., Arzilli, F., Daga, R., Caselli, A., Reckziegel, F., Viramonte, J., Díaz-Alvarado, J., Polacci, M., Burton, M., and Perugini, D.: Eruption dynamics of the 22-23 April 2015 Calbuco Volcano

(Southern Chile): Analyses of tephra fall deposits, Journal of Volcanology and Geothermal Research, 317, 15–29, doi:10.1016/j.jvolgeores.2016.02.027, http://dx.doi.org/10.1016/j.jvolgeores.2016.02.027, 2016.

Schneising, O., Bergamaschi, P., Bovensmann, H., Buchwitz, M., Burrows, J. P., Deutscher, N. M., Griffith, D. W. T., Heymann, J., Macatangay, R., Messerschmidt, J., Notholt, J., Rettinger, M., Reuter, M., Sussmann, R., Velazco, V. A., Warneke, T., Wennberg, P. O., and Wunch, D.: Atmospheric greenhouse gases retrieved from SCIAMACHY: comparison to ground-based FTS measurements and model results, Atmospheric Chemistry and Physics, 12, 1527–1540, doi:10.5194/acp-12-1527-2012, http://www.atmos-chem-phys.net/12/1527/2012/, 2012.

Sherlock, V., Connor, B. J., Robinson, J., Shiona, H., Smale, D., and Pollard, D.: TCCON data from Lauder, New Zealand, 125HR, Release GGG2014R0, TCCON data archive, hosted by the Carbon Dioxide Information Analysis Center, Oak Ridge National Laboratory, Oak Ridge, Tennessee, U.S.A., http://dx.doi.org/10.14291/tccon.ggg2014.lauder02.R0/1149298, doi:10.14291/tccon.ggg2014.lauder02.R0/1149298, 2014.

Singh, H. B., Brune, W. H., Crawford, J. H., Jacob, D. J., and Russell, P. B.: Overview of the summer 2004 Intercontinental Chemical Transport Experiment-North America (INTEX-A), Journal of Geophysical Research: Atmospheres, 111, doi:10.1029/2006JD007905, 2006.

Strong, K., Mendonca, J., Weaver, D., Fogal, P., Drummond, J., Batchelor, R., and Lindenmaier, R.: TCCON data from Eureka, Canada, Release GGG2014R0, TCCON data archive, hosted by the Carbon Dioxide Information Analysis Center, Oak Ridge National Laboratory, Oak Ridge, Tennessee, U.S.A., http://dx.doi.org/10.14291/tccon.ggg2014.eureka01.R0/1149271, doi:10.14291/tccon.ggg2014.eureka01.R0/1149271, 2014.

Sussmann, R. and Rettinger, M.: TCCON data from Garmisch, Germany, Release GGG2014R0, TCCON data archive, hosted by the Carbon Dioxide Information Analysis Center, Oak Ridge National Laboratory, Oak Ridge, Tennessee, U.S.A., http://dx.doi.org/10.14291/tccon.ggg2014.garmisch01.R0/1149299, doi:10.14291/tccon.ggg2014.garmisch01.R0/1149299, 2014.

Te, Y., Jeseck, P., and Janssen, C.: TCCON data from Paris, France, Release GGG2014R0, TCCON data archive, hosted by the Carbon Dioxide Information Analysis Center, Oak Ridge National Laboratory, Oak Ridge, Tennessee, U.S.A., http://dx.doi.org/10.14291/tccon.ggg2014.paris01.R0/1149279, doi:10.14291/tccon.ggg2014.paris01.R0/1149279, 2014.

Warneke, T., Messerschmidt, J., Notholt, J., Weinzierl, C., Deutscher, N. M., Petri, C., Grupe, P., Vuillemin, C., Truong, F., Schmidt, M., Ramonet, M., and Parmentier, E.: TCCON data from Orleans, France, Release GGG2014R0, TCCON data archive, hosted by the Carbon Dioxide Information Analysis Center, Oak Ridge National Laboratory, Oak Ridge, Tennessee, U.S.A., http://dx.doi.org/10.14291/tccon.ggg2014.orleans01.R0/1149276, doi:10.14291/tccon.ggg2014.orleans01.R0/1149276, 2014.

Wennberg, P. O., Roehl, C., Wunch, D., Toon, G. C., Blavier, J.-F., Washenfelder, R., Keppel-Aleks, G., Allen, N., and Ayers, J.: TCCON data from Park Falls, Wisconsin, USA, Release GGG2014R0, TCCON data archive, hosted by the Carbon Dioxide Information Analysis Center, Oak Ridge National Laboratory, Oak Ridge, Tennessee, U.S.A., http://dx.doi.org/10.14291/tccon.ggg2014.parkfalls01.R0/1149161, doi:10.14291/tccon.ggg2014.parkfalls01.R0/1149161, 2014a.

Wennberg, P. O., Wunch, D., Roehl, C., Blavier, J.-F., Toon, G. C., Allen, N., Dowell, P., Teske, K., Martin, C., and Martin., J.: TCCON data from Lamont, Oklahoma, USA, Release GGG2014R0, TCCON data archive, hosted by the Carbon Dioxide Information Analysis Center, Oak Ridge National Laboratory, Oak Ridge, Tennessee, U.S.A., http://dx.doi.org/10.14291/tccon.ggg2014.lamont01.R0/1149159, doi:10.14291/tccon.ggg2014.lamont01.R0/1149159, 2014b.

Wennberg, P. O., Wunch, D., Roehl, C., Blavier, J.-F. L., Toon, G. C., and Allen, N.: TCCON data from California Institute of Technology, Pasadena, California, USA, Release GGG2014R1, TCCON data archive, hosted by the Carbon Dioxide Information Analysis Center, Oak Ridge National Laboratory, Oak Ridge, Tennessee, U.S.A., http://dx.doi.org/10.14291/tccon.ggg2014.pasadena01.R1/1182415, doi:10.14291/tccon.ggg2014.pasadena01.R1/1182415, 2014c.

Wofsy, S. C.: HIAPER Pole-to-Pole Observations (HIPPO): fine-grained, global-scale measurements of climatically important atmospheric gases and aerosols., Philosophical Transactions of the Royal Society - Series A: Mathematical, Physical and Engineering Sciences, 369, 2073–86, doi:10.1098/rsta.2010.0313, http://www.ncbi.nlm.nih.gov/pubmed/21502177, 2011.

Wunch, D., Toon, G. C., Wennberg, P. O., Wofsy, S. C., Stephens, B. B., Fischer, M. L., Uchino, O., Abshire, J. B., Bernath, P. F., Biraud, S. C., Blavier, J.-F. L., Boone, C., Bowman, K. P., Browell, E. V., Campos, T., Connor, B. J., Daube, B. C., Deutscher, N. M., Diao, M., Elkins, J. W., Gerbig, C., Gottlieb, E., Griffith, D. W. T., Hurst, D. F., Jiménez, R., Keppel-Aleks, G., Kort, E. A., MacAtangay, R., MacHida, T., Matsueda, H., Moore, F., Morino, I., Park, S., Robinson, J., Roehl, C. M., Sawa, Y., Sherlock, V., Sweeney, C., Tanaka, T., and Zondlo, M. a.: Calibration of the total carbon column observing network using aircraft profile data, Atmospheric Measurement Techniques, 3, 1351–1362, doi:10.5194/amt-3-1351-2010, http://www.atmos-meas-tech.net/3/1351/2010/, 2010.

Wunch, D., Toon, G. C., Blavier, J.-F. L., Washenfelder, R. A., Notholt, J., Connor, B. J., Griffith, D. W. T., Sherlock, V., and Wennberg, P. O.: The total carbon column observing network., Philosophical transactions. Series A, Mathematical, physical, and engineering sciences, 369, 2087–2112, doi:10.1098/rsta.2010.0240, http://rsta.royalsocietypublishing.org/content/369/1943/2087http://www.ncbi.nlm.nih.gov/pubmed/21502178, 2011a.

Wunch, D., Wennberg, P. O., Toon, G. C., Connor, B. J., Fisher, B., Osterman, G. B., Frankenberg, C., Mandrake, L., O'Dell, C. W., Ahonen, P., Biraud, S. C., Castano, R., Cressie, N., Crisp, D., Deutscher, N. M., Eldering, A., Fisher, M. L., Griffith, D. W. T., Gunson, M., Heikkinen, P., Keppel-Aleks, G., Kyrö, E., Lindenmaier, R., MacAtangay, R., Mendonca, J., Messerschmidt, J., Miller, C. E., Morino, I., Notholt, J., Oyafuso, F. A., Rettinger, M., Robinson, J., Roehl, C. M., Salawitch, R. J., Sherlock, V., Strong, K., Sussmann, R., Tanaka, T., Thompson, D. R., Uchino, O., Warneke, T., and Wofsy, S. C.: A method for evaluating bias in global measurements of CO2 total columns from space, Atmospheric Chemistry and Physics, 11, 12 317–12 337, doi:10.5194/acp-11-12317-2011, http://www.atmos-chem-phys.net/11/12317/2011/, 2011b.

Wunch, D., Toon, G. C., Sherlock, V., Deutscher, N. M., Liu, C., Feist, D. G., and Wennberg, P. O.: The Total Carbon Column Observing Network's GGG2014 Data Version, Tech. rep., California Institute of Technology, Carbon Dioxide Information Analysis Center, Oak Ridge National Laboratory, Oak Ridge, Tennessee, U.S.A. doi: 10.14291/tccon.ggg2014.documentation.R0/1221662,

doi:10.14291/tccon.ggg2014.documentation.R0/1221662, http://dx.doi.org/10.14291/tccon.ggg2014.documentation.R0/1221662, 2015.

Yang, Z., Washenfelder, R. a., Keppel-Aleks, G., Krakauer, N. Y., Randerson, J. T., Tans, P. P., Sweeney, C., and Wennberg, P. O.: New constraints on Northern Hemisphere growing season net flux, Geophysical Research Letters, 34, L12 807, doi:10.1029/2007GL029742, http://www.agu.org/pubs/crossref/2007/2007GL029742.shtml, 2007.

York, D., Evensen, N. M., Martinez, M. L., and De Basabe Delgado, J.: Unified equations for the slope, intercept, and standard errors of the best straight line, American Journal of Physics, 72, 367, doi:10.1119/1.1632486, http://link.aip.org/link/AJPIAS/v72/i3/p367/s1{&}Agg=doi, 2004.

Zhao, C. L. and Tans, P. P.: Estimating uncertainty of the WMO mole fraction scale for carbon dioxide in air, Journal of Geophysical Research, 111, 1–10, doi:10.1029/2005JD006003, http://www.agu.org/pubs/crossref/2006/2005JD006003.shtml, 2006.

Atmos. Meas. Tech. Discuss., doi:10.5194/amt-2016-227, 2016
Manuscript under review for journal Atmos. Meas. Tech.
Published: 29 August 2016

Atmospheric Measurement Techniques Discussions

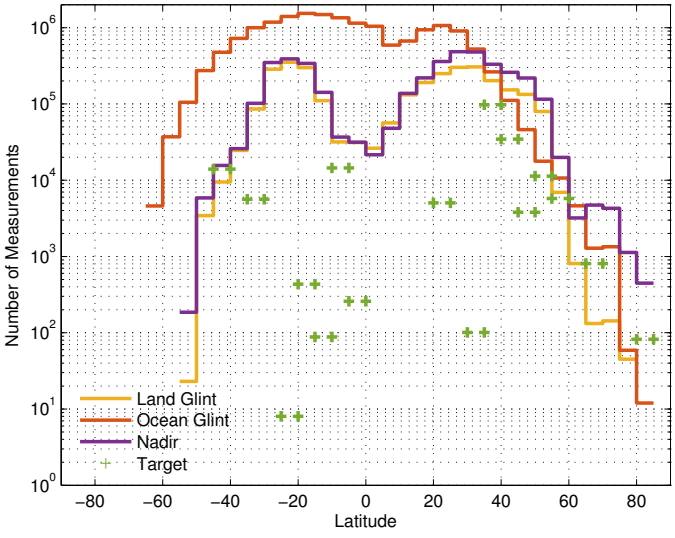

Figure 1: Nadir, and glint, and target-mode measurement density in 5° bins as a function of latitude from the beginning of the mission through April 30, 2016. These are from the "lite" files applying "warn level" 11 filters and requiring that the "outcome_flag" is zero.

Atmos. Meas. Tech. Discuss., doi:10.5194/amt-2016-227, 2016
Manuscript under review for journal Atmos. Meas. Tech.
Published: 29 August 2016

Atmospheric Measurement Techniques Discussions

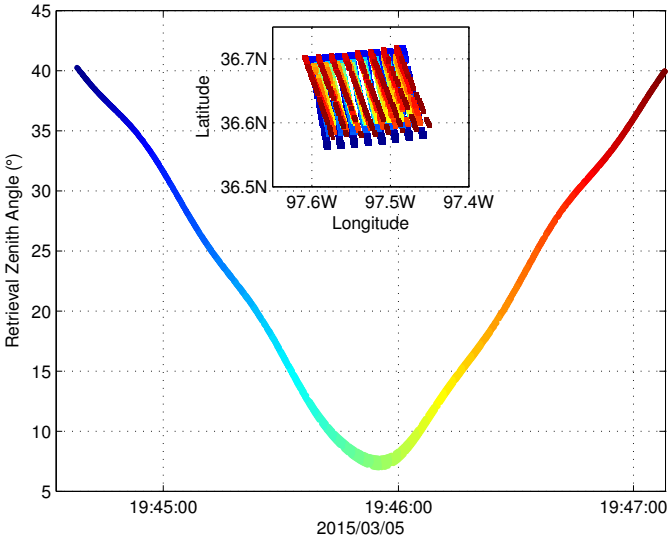

Figure 2: The zenith angles viewed during a target mode measurement over Lamont. The spacecraft "nods" across the ground target as it rotates overhead. The colours represent the time of the measurement. The top inset shows the locations of the measurements in latitude and longitude.

Figure 3: Map of OCO-2 target locations. Gold circles show the locations of the targets that coincide with TCCON stations; orange stars show the locations of targets that do not have co-located TCCON stations.

Atmos. Meas. Tech. Discuss., doi:10.5194/amt-2016-227, 2016
Manuscript under review for journal Atmos. Meas. Tech.
Published: 29 August 2016

Atmospheric Measurement Techniques Discussions

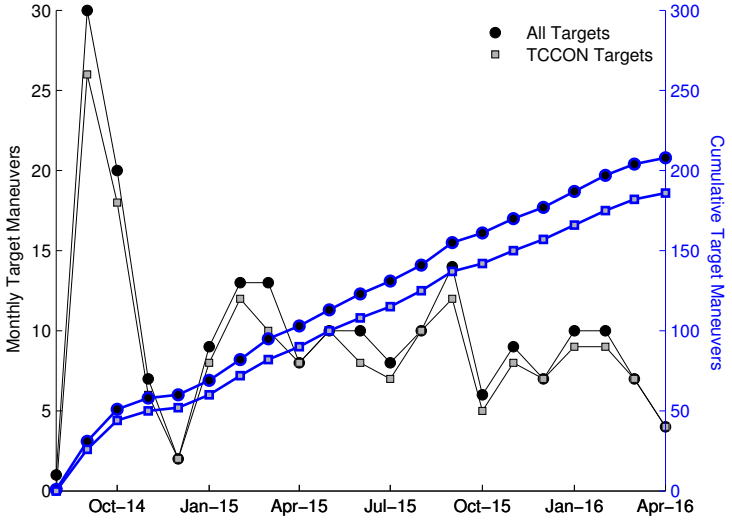

Figure 4: The number of target mode maneuvers attempted per month (left axis), and the cumulative number of target mode maneuvers attempted to date (right axis). The TCCON targets are in grey squares; all targets (including Railroad Valley, which does not have a TCCON station) are marked in black circles.

Atmos. Meas. Tech. Discuss., doi:10.5194/amt-2016-227, 2016
Manuscript under review for journal Atmos. Meas. Tech.
Published: 29 August 2016

Atmospheric Measurement Techniques Discussions

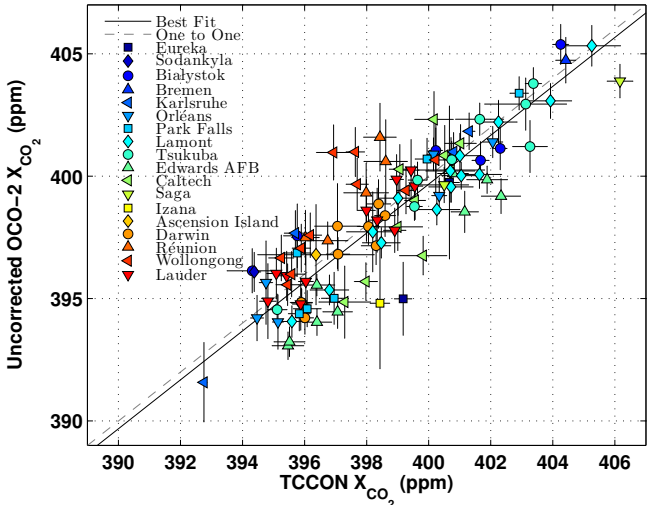

(a) Without bias correction.

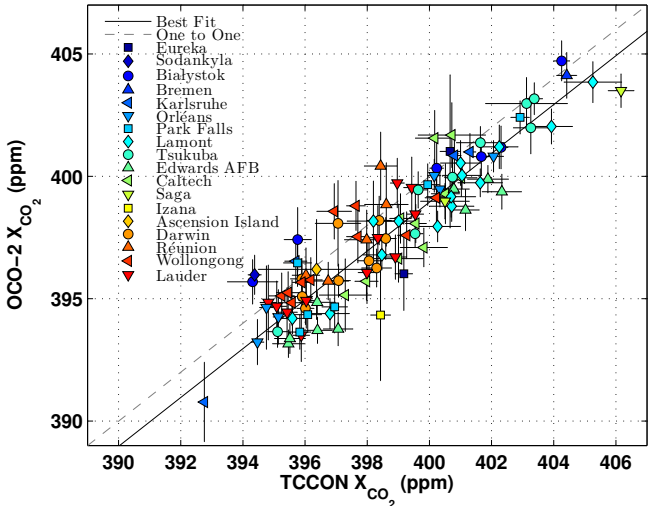

(b) With bias correction.

Figure 5: The relationship between the OCO-2 target-mode data and the coincident TCCON data. The top plot (a) does not have the Mandrake et al. (2015) bias correction applied, the bottom plot (b) is after bias correction, but before the scaling is applied. The one-to-one line is indicated by the dashed black line, and the best fit is marked in the solid black line.

Atmos. Meas. Tech. Discuss., doi:10.5194/amt-2016-227, 2016
Manuscript under review for journal Atmos. Meas. Tech.
Published: 29 August 2016

Atmospheric Measurement Techniques Discussions

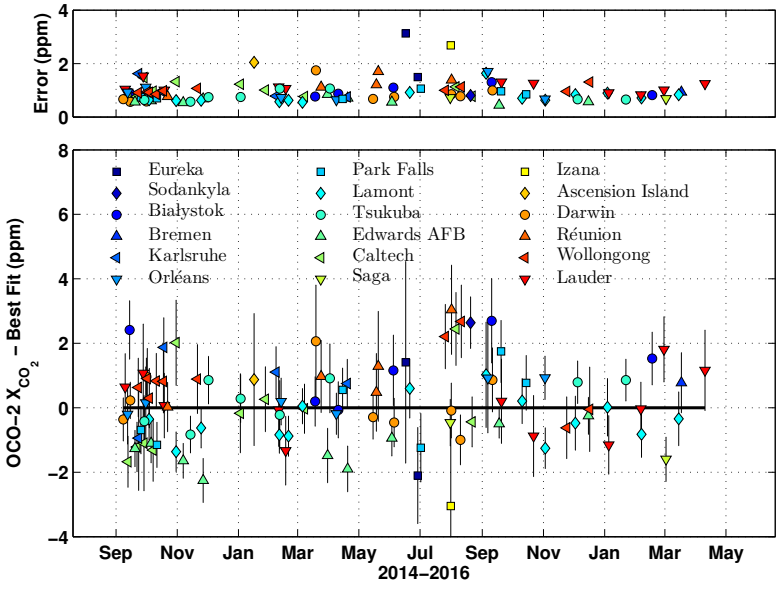

Figure 6: The time series of the differences between the OCO-2 target-mode data and the best fit line in Fig. 5(b). The top panel shows the magnitude of the sum in quadrature of the standard deviation of the OCO-2 data during the target and the standard deviation of the coincident TCCON data. Those values are plotted as the error bars in the lower panel.

Atmos. Meas. Tech. Discuss., doi:10.5194/amt-2016-227, 2016
Manuscript under review for journal Atmos. Meas. Tech.
Published: 29 August 2016

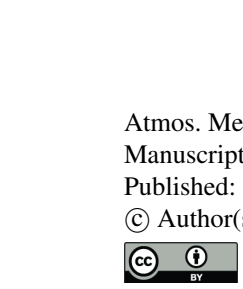

Atmospheric Measurement Techniques Discussions

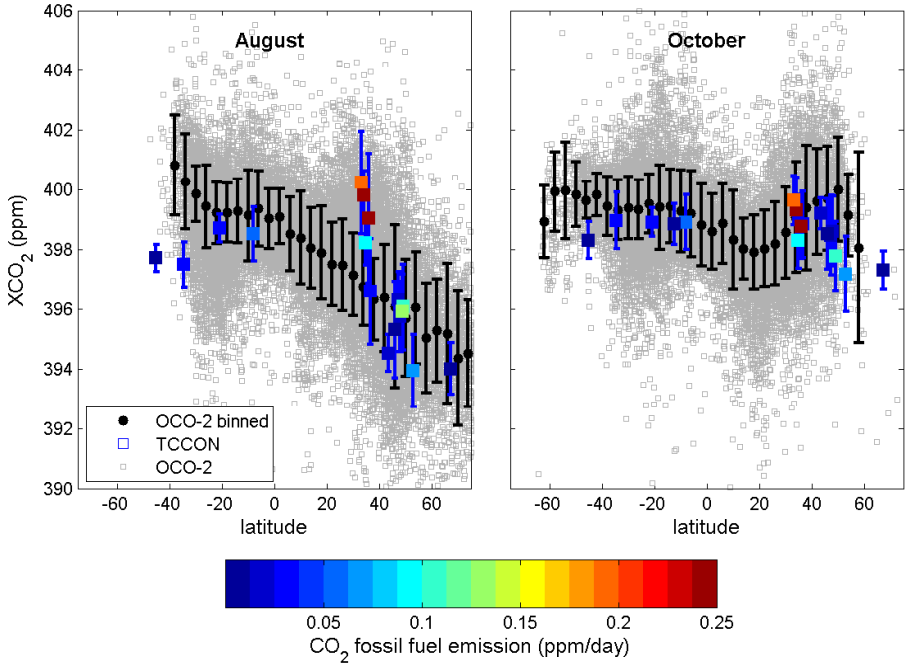

Figure 7: The latitudinal gradient of OCO-2 data in August 2015 (left), and in October 2015 (right). The grey squares are monthly mean OCO-2 data from glint and nadir mode gridded in $0.5°\times0.5°$ bins. The black circles are the OCO-2 zonal means after gridding onto a $4°\times5°$ grid. The error bars indicate the 1σ standard deviation. The TCCON monthly medians are marked by the squares with 1σ standard deviation error bars. The colours represent the CO_2 fossil fuel emissions within 50 km of the TCCON location. The fossil fuel emission source is from the European Commission, Joint Research Centre (JRC)/Netherlands Environmental Assessment Agency (PBL). Emission Database for Global Atmospheric Research (EDGAR), http://edgar.jrc.ec.europe.eu. The high bias of the OCO-2 data in the higher latitude southern hemisphere (which is dominated by glint measurements over water) is clearly evident in the August plot south of -20°.

Atmos. Meas. Tech. Discuss., doi:10.5194/amt-2016-227, 2016
Manuscript under review for journal Atmos. Meas. Tech.
Published: 29 August 2016

Atmospheric Measurement Techniques Discussions

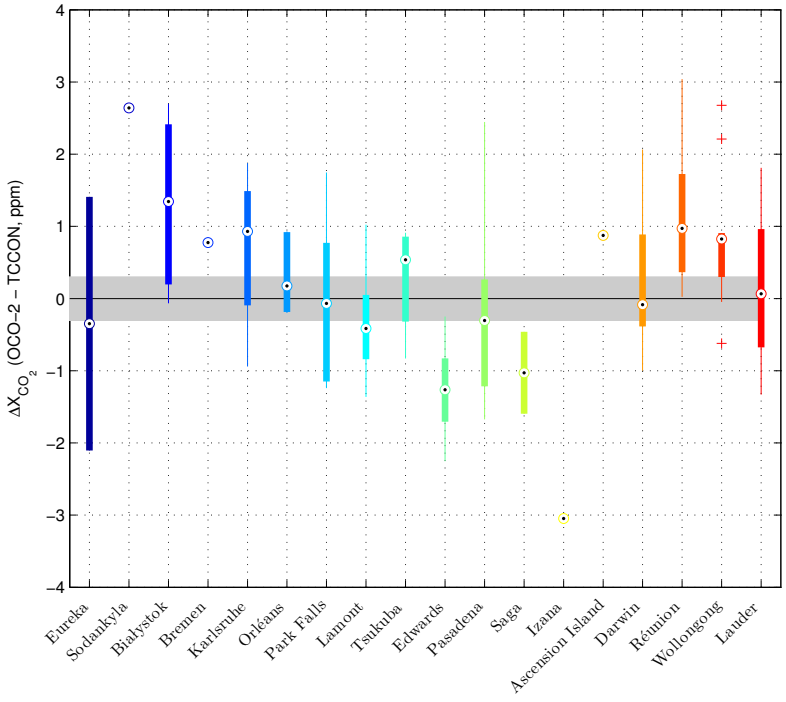

Figure 8: The site-to-site differences between the OCO-2 target-mode data and the coincident TCCON data. This is a "box plot": the circles indicate the median value of the difference, the thick bars indicate the 25 and 75 percentile limits, the thin bars represent the full range of the data, excluding the outliers (McGill et al., 1978). The outliers are represented by plus ('+') symbols. The grey shaded area indicates the ± 0.3 ppm uncertainty in the TCCON values: deviations beyond the shading can be attributed to uncertainties in the OCO-2 data.

Atmos. Meas. Tech. Discuss., doi:10.5194/amt-2016-227, 2016
Manuscript under review for journal Atmos. Meas. Tech.
Published: 29 August 2016

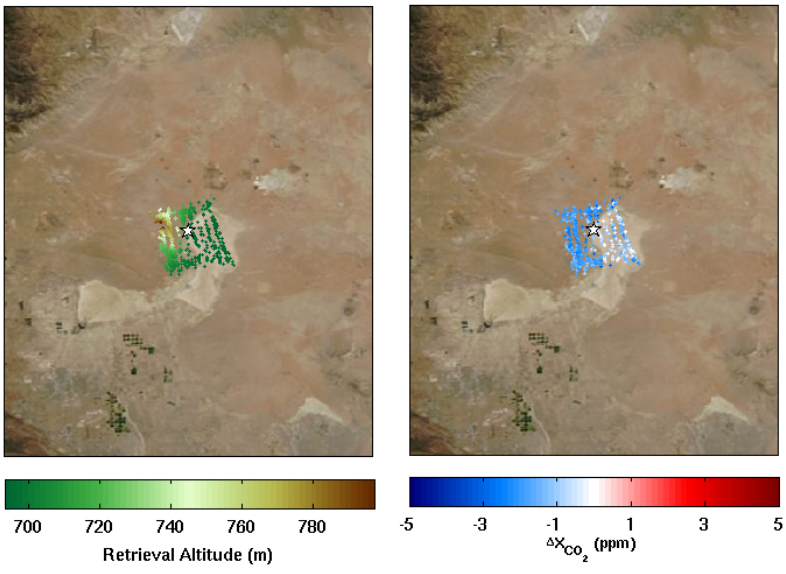

Figure 9: Edwards target on April 19, 2015. The background is the MODIS true-colour image of the Edwards area at the time of the target-mode measurements. The white star indicates the location of the Edwards TCCON station. The left panel shows the elevation model of the surface and the right panel shows the difference in OCO-2 X_{CO_2} from the value recorded by the TCCON instrument. A spatial bias related to the surface brightness is clearly present in this target-mode measurement. In other Edwards target mode measurements, this surface brightness-correlated bias is not as apparent.

Atmos. Meas. Tech. Discuss., doi:10.5194/amt-2016-227, 2016
Manuscript under review for journal Atmos. Meas. Tech.
Published: 29 August 2016

Atmospheric Measurement Techniques Discussions

Figure 10: The retrieval altitudes near the Wollongong TCCON station during target measurements. The sharp Illawarra escarpment can be clearly seen inland from the Tasman Sea (to the East).

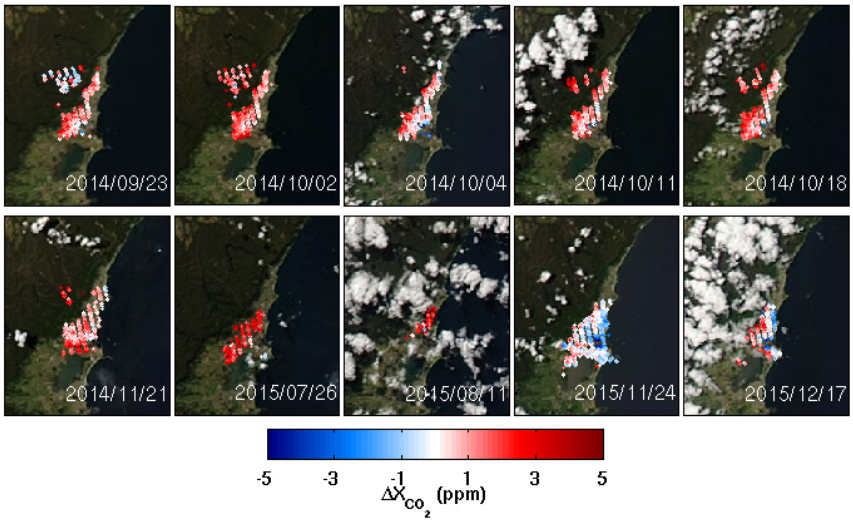

Figure 11: The filtered target-mode measurements over Wollongong. The colours represent the difference between the OCO-2 measurement and the coincident TCCON measurement. The OCO-2 data over Wollongong are generally higher (redder) than the TCCON measurements, and significantly high in the July and August 2015 target-mode maneuvers.

Atmos. Meas. Tech. Discuss., doi:10.5194/amt-2016-227, 2016
Manuscript under review for journal Atmos. Meas. Tech.
Published: 29 August 2016

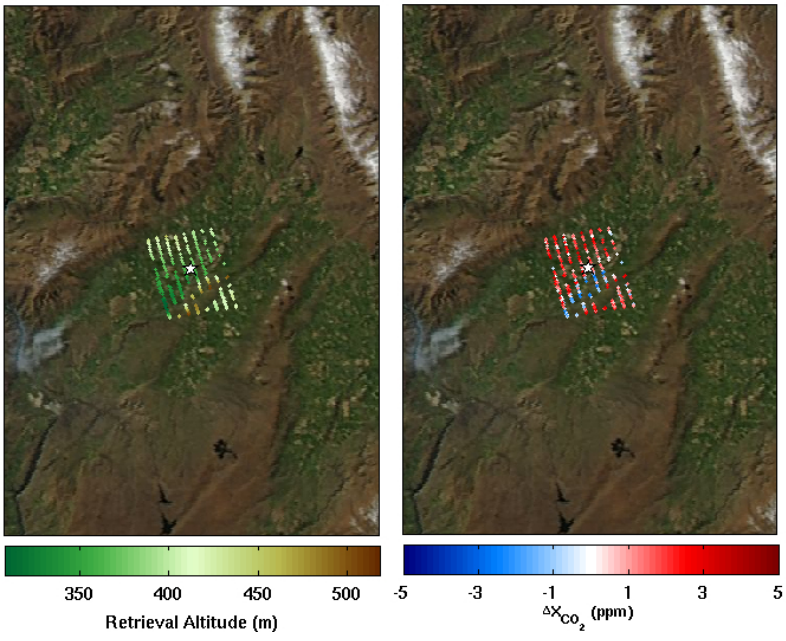

Figure 12: Lauder target on September 28, 2014. The background is the MODIS true-colour image of the Lauder area at the time of the target-mode measurements. The white star indicates the location of the Lauder TCCON station. The left panel shows the elevation model of the surface and the right panel shows the difference in X_{CO_2} from the value recorded by the TCCON instrument. A spatial bias is clearly present, related to the surface elevation.

Atmos. Meas. Tech. Discuss., doi:10.5194/amt-2016-227, 2016
Manuscript under review for journal Atmos. Meas. Tech.
Published: 29 August 2016

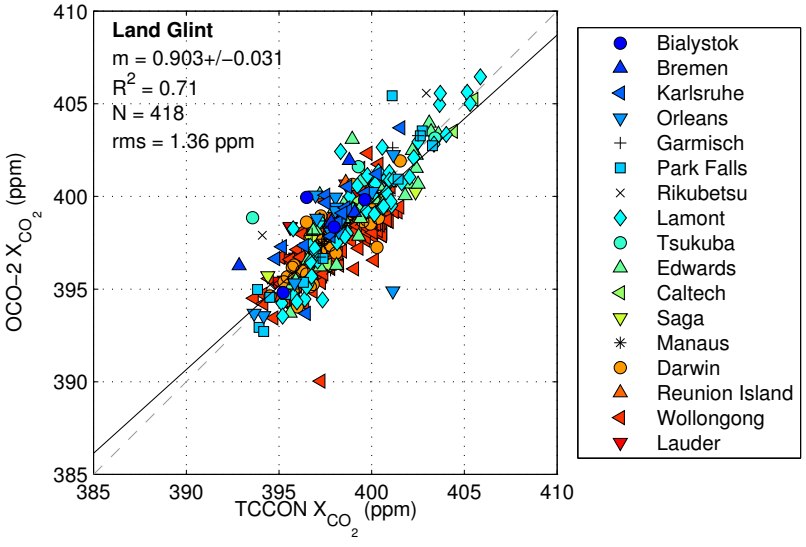

Figure 13: Land glint OCO-2 one-to-one plot against TCCON. The slope of the relationship is represented by "m" in the figure, and the coefficient of determination is represented by "R^2". The number of points on the graph is indicated by "N" and the root-mean-square value (rms) of the differences between OCO-2 and TCCON X_{CO_2} is also shown.

Atmos. Meas. Tech. Discuss., doi:10.5194/amt-2016-227, 2016
Manuscript under review for journal Atmos. Meas. Tech.
Published: 29 August 2016

Atmospheric Measurement Techniques Discussions

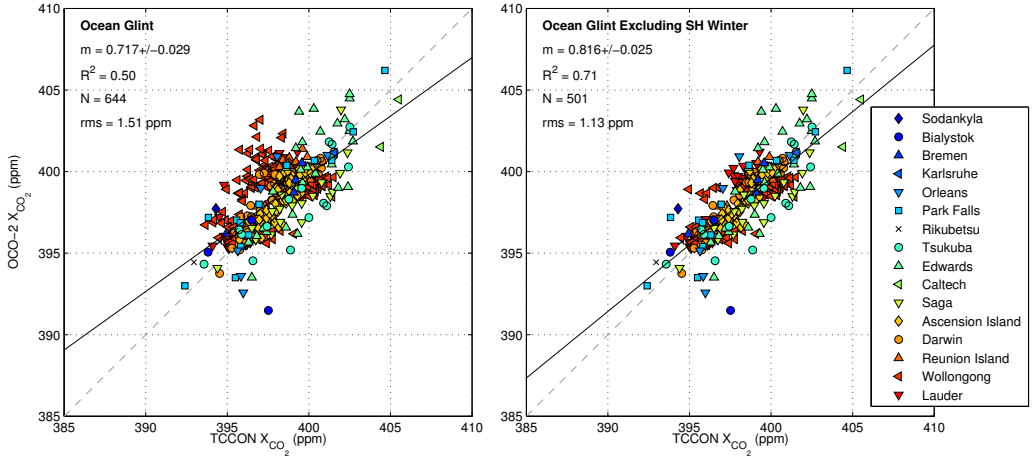

Figure 14: Ocean glint OCO-2 one-to-one plot against TCCON. The left panel shows all the glint-mode data. The right panel removes the southern hemisphere wintertime (June through September) glint data that has a known high bias.

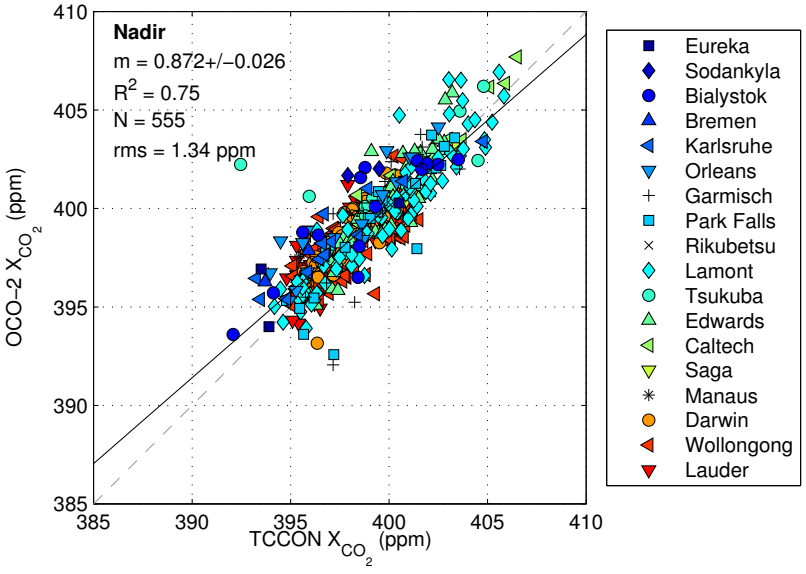

Figure 15: Nadir OCO-2 one-to-one plot against TCCON.

Atmos. Meas. Tech. Discuss., doi:10.5194/amt-2016-227, 2016
Manuscript under review for journal Atmos. Meas. Tech.
Published: 29 August 2016

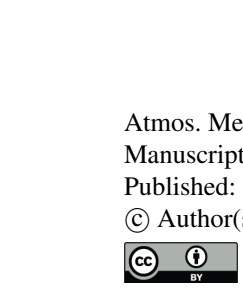

Atmospheric Measurement Techniques Discussions

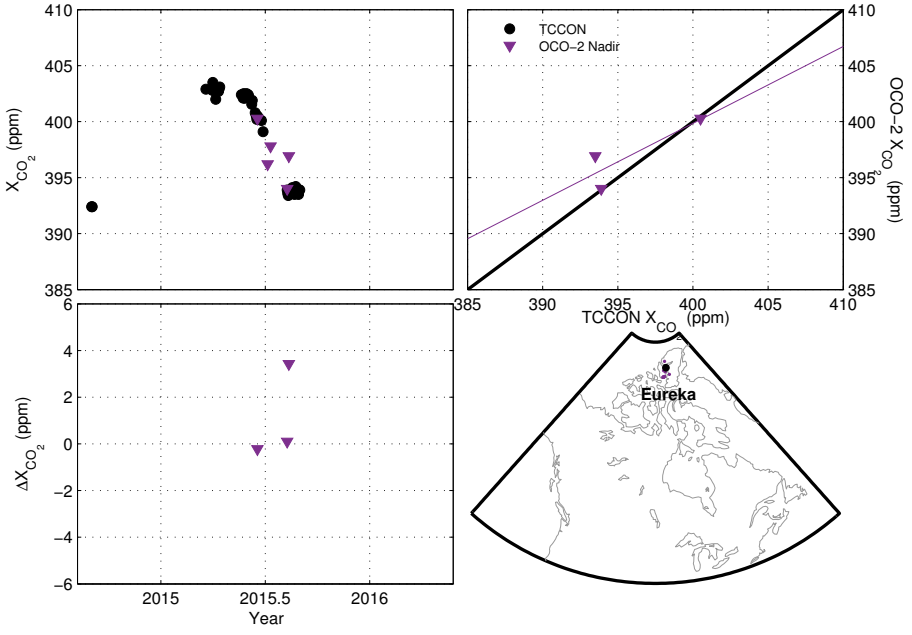

(a) Eureka

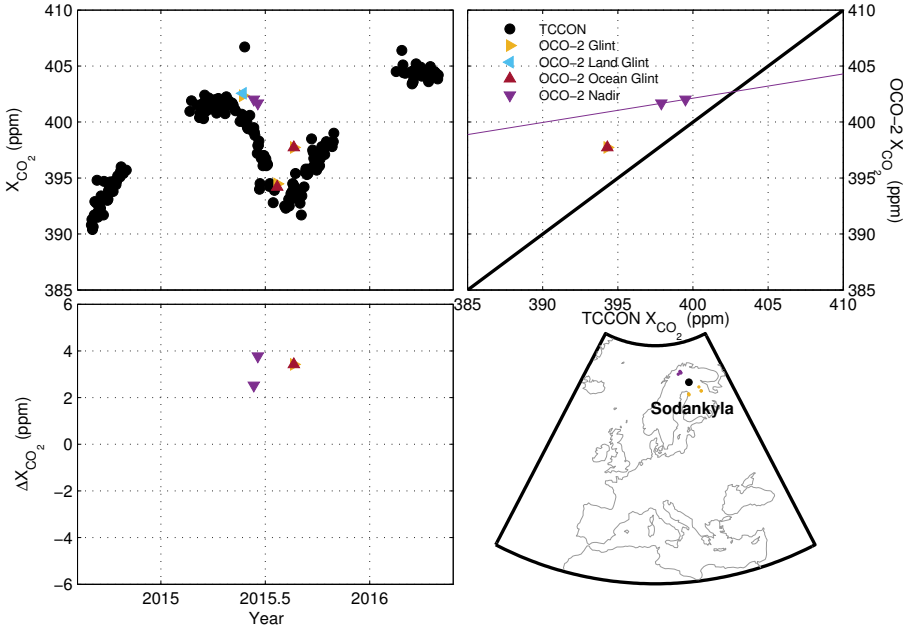

(b) Sodankylä

Atmos. Meas. Tech. Discuss., doi:10.5194/amt-2016-227, 2016
Manuscript under review for journal Atmos. Meas. Tech.
Published: 29 August 2016

Atmospheric Measurement Techniques Discussions

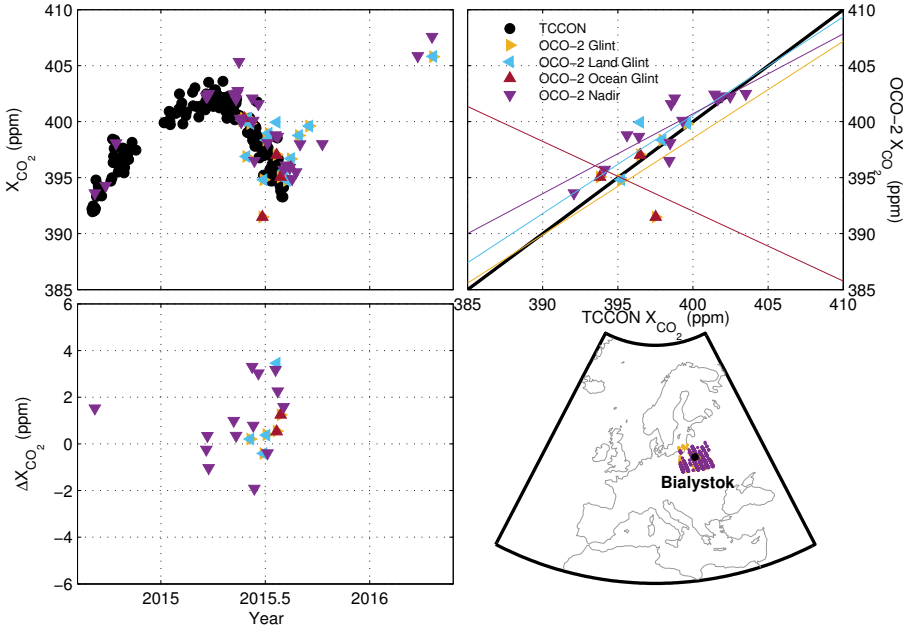

(c) Białystok

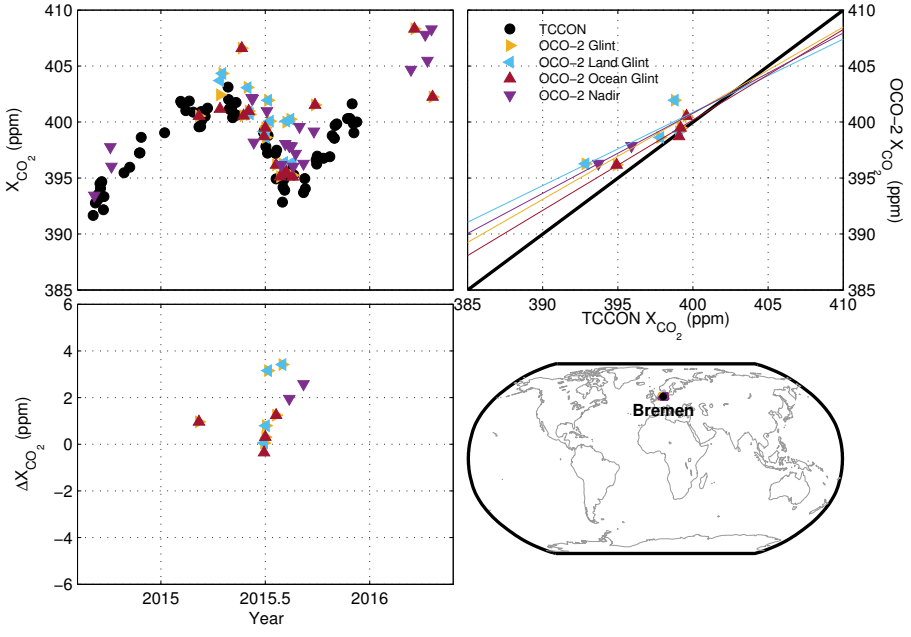

(d) Bremen

Atmos. Meas. Tech. Discuss., doi:10.5194/amt-2016-227, 2016
Manuscript under review for journal Atmos. Meas. Tech.
Published: 29 August 2016

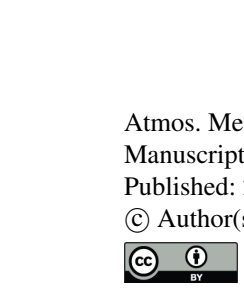

Atmospheric Measurement Techniques Discussions

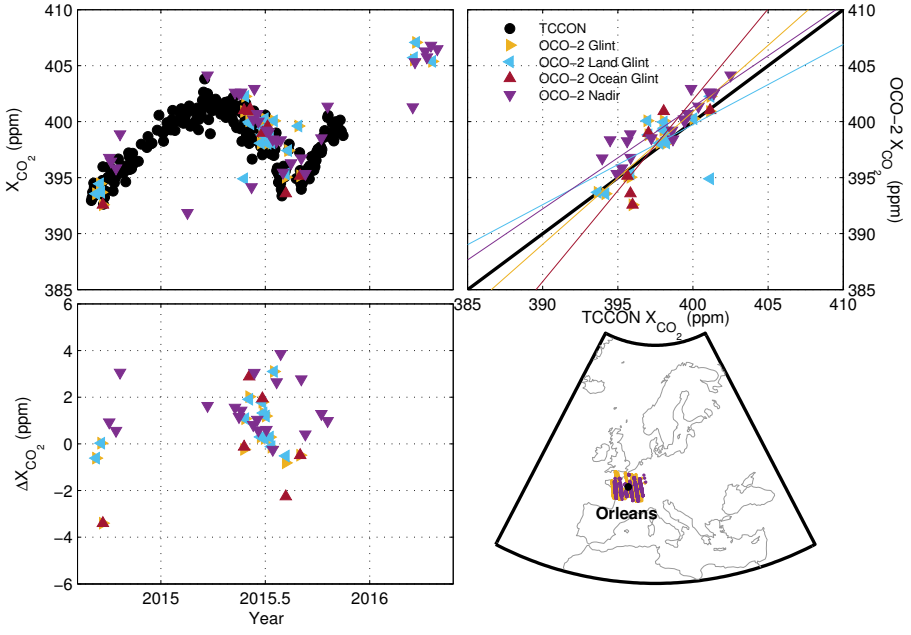

(e) Orléans

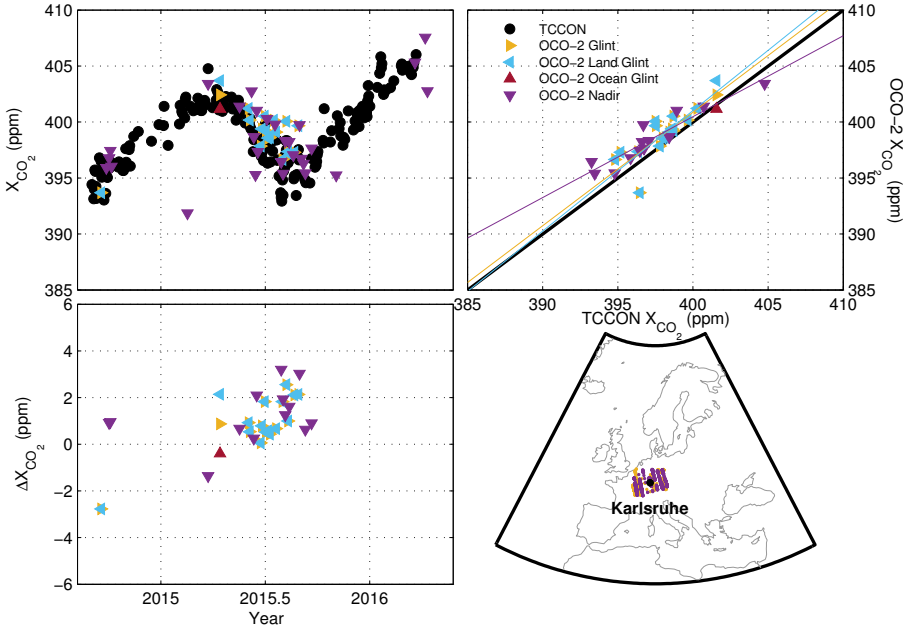

(f) Karlsruhe

Atmos. Meas. Tech. Discuss., doi:10.5194/amt-2016-227, 2016
Manuscript under review for journal Atmos. Meas. Tech.
Published: 29 August 2016

Atmospheric Measurement Techniques Discussions

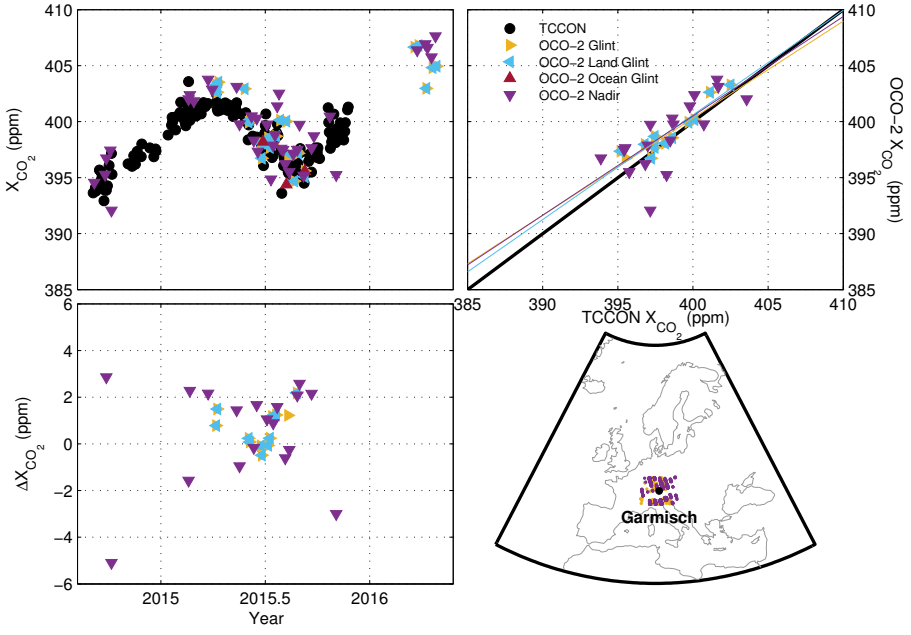

(g) Garmisch: Sussmann and Rettinger (2014)

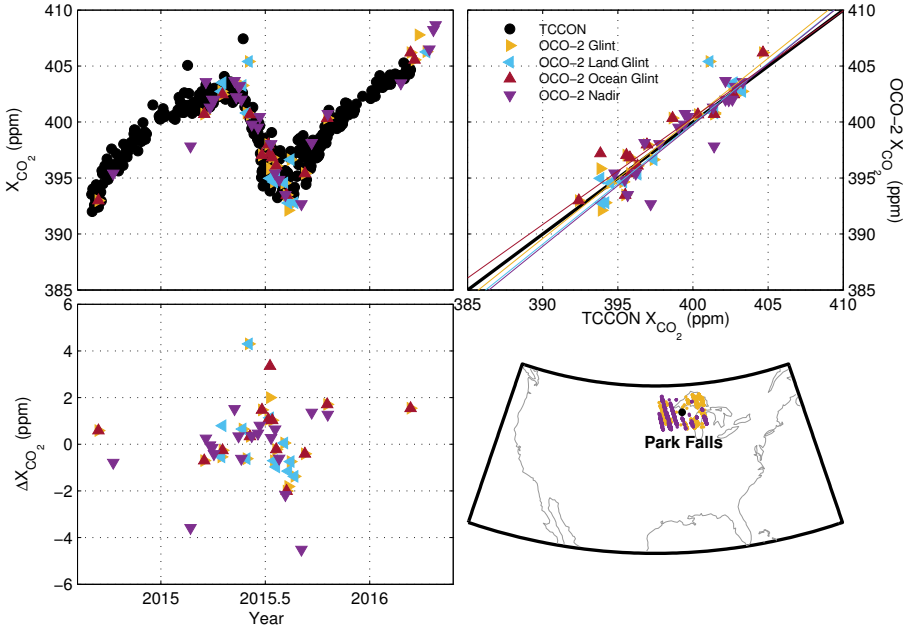

(h) Park Falls

Atmos. Meas. Tech. Discuss., doi:10.5194/amt-2016-227, 2016
Manuscript under review for journal Atmos. Meas. Tech.
Published: 29 August 2016

Atmospheric Measurement Techniques Discussions

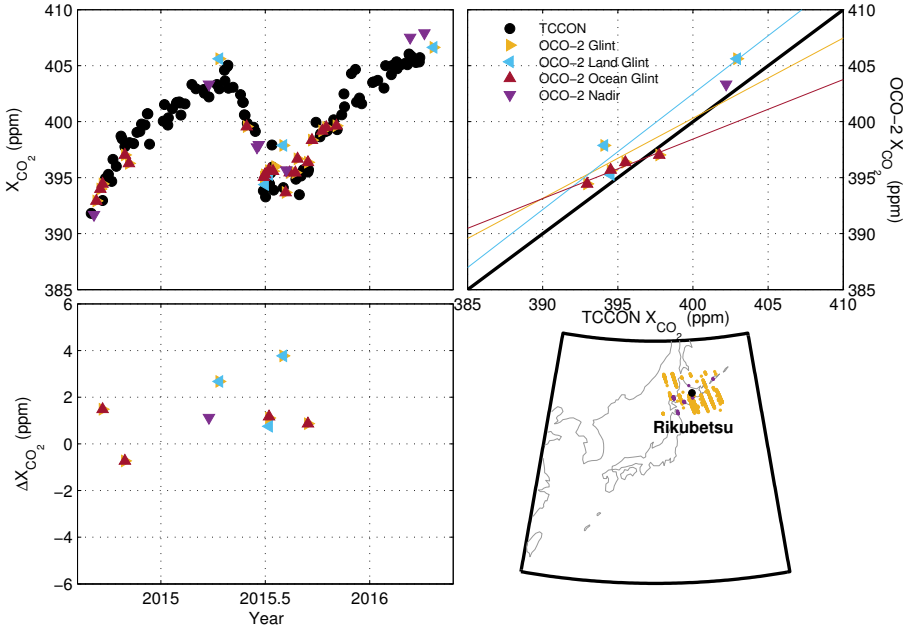

(i) Rikubetsu

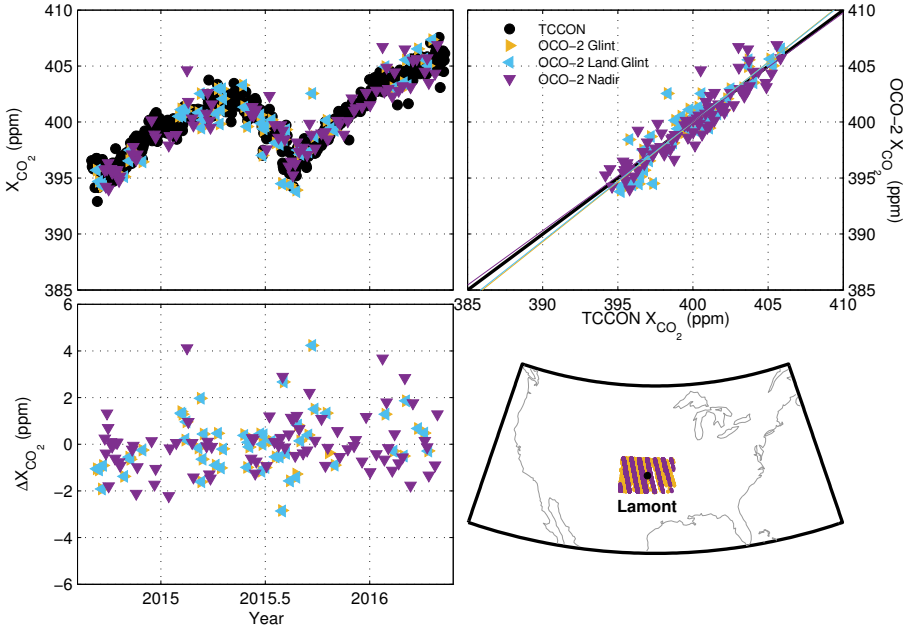

(j) Lamont

Atmos. Meas. Tech. Discuss., doi:10.5194/amt-2016-227, 2016
Manuscript under review for journal Atmos. Meas. Tech.
Published: 29 August 2016

Atmospheric Measurement Techniques Discussions

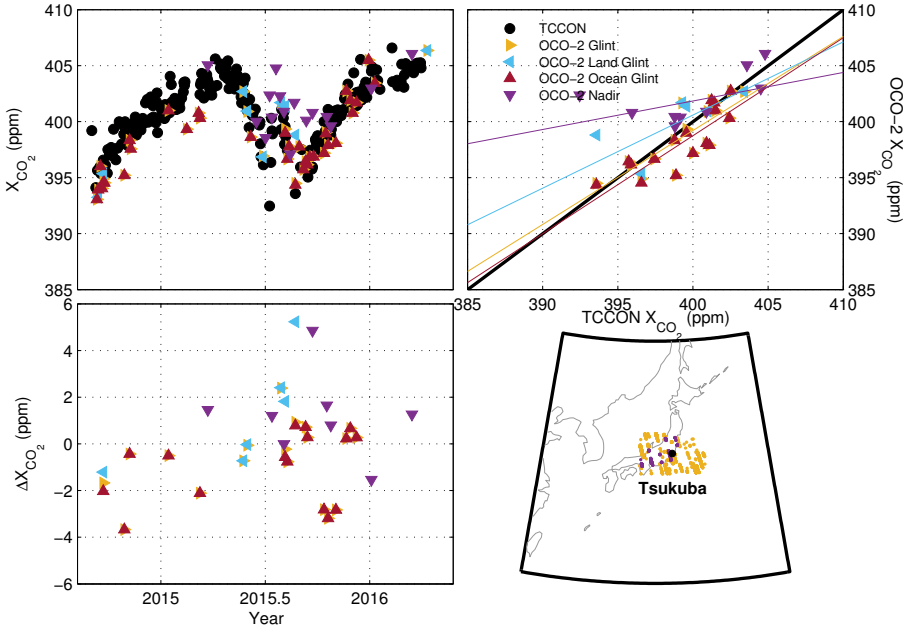

(k) Tsukuba

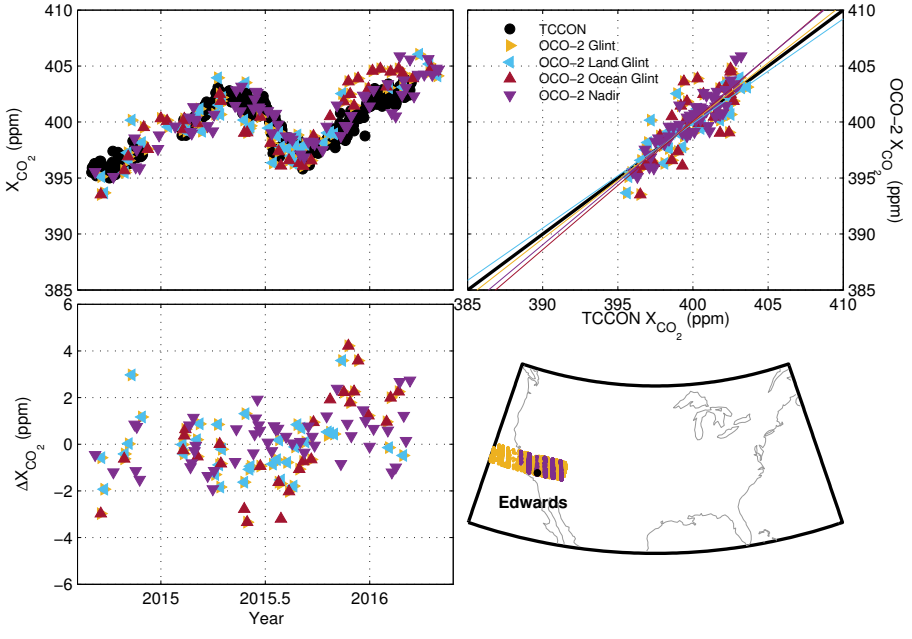

(l) Edwards

Atmos. Meas. Tech. Discuss., doi:10.5194/amt-2016-227, 2016
Manuscript under review for journal Atmos. Meas. Tech.
Published: 29 August 2016

Atmospheric Measurement Techniques Discussions

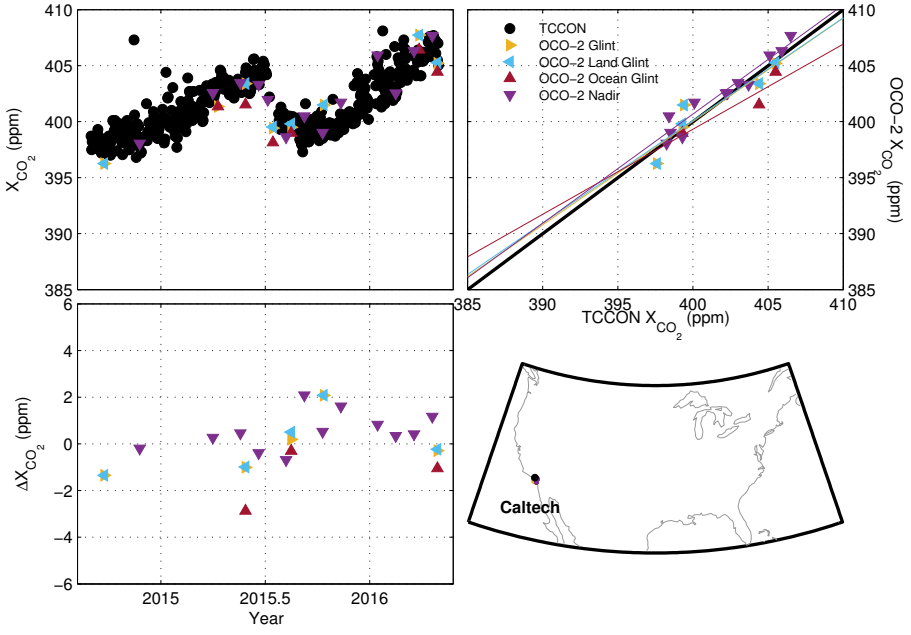

(m) Pasadena

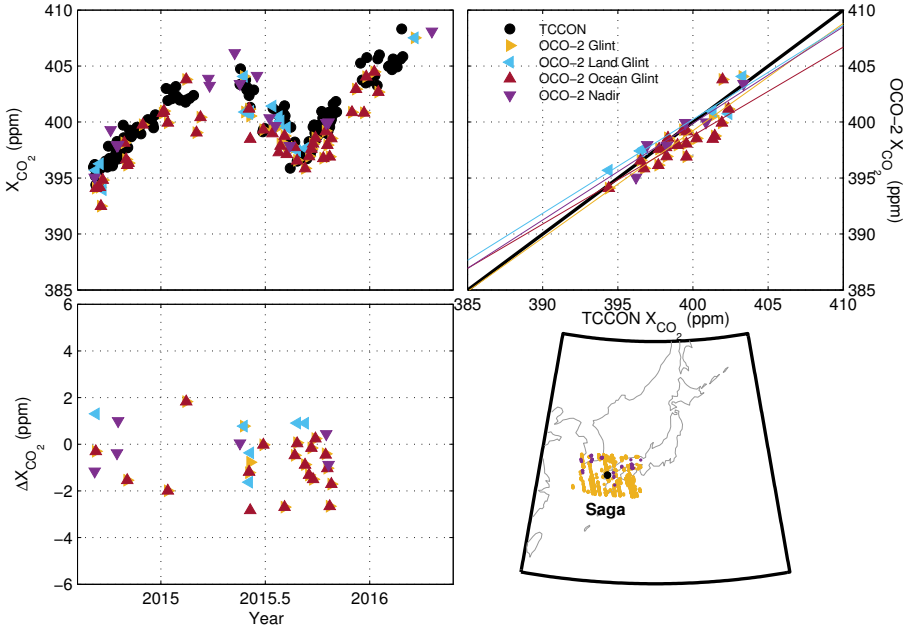

(n) Saga

Atmos. Meas. Tech. Discuss., doi:10.5194/amt-2016-227, 2016
Manuscript under review for journal Atmos. Meas. Tech.
Published: 29 August 2016

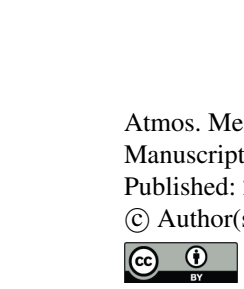

Atmospheric Measurement Techniques Discussions

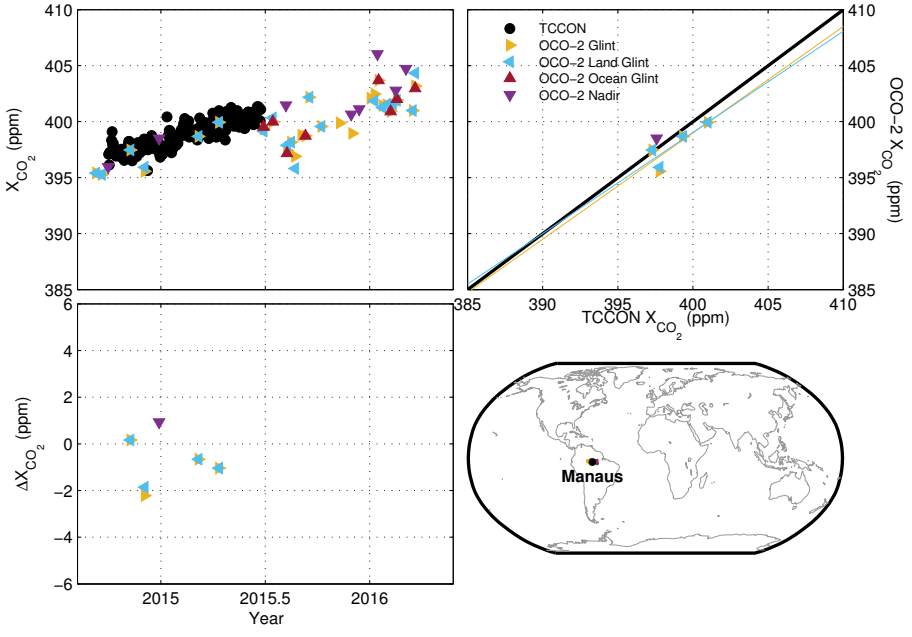

(o) Manaus

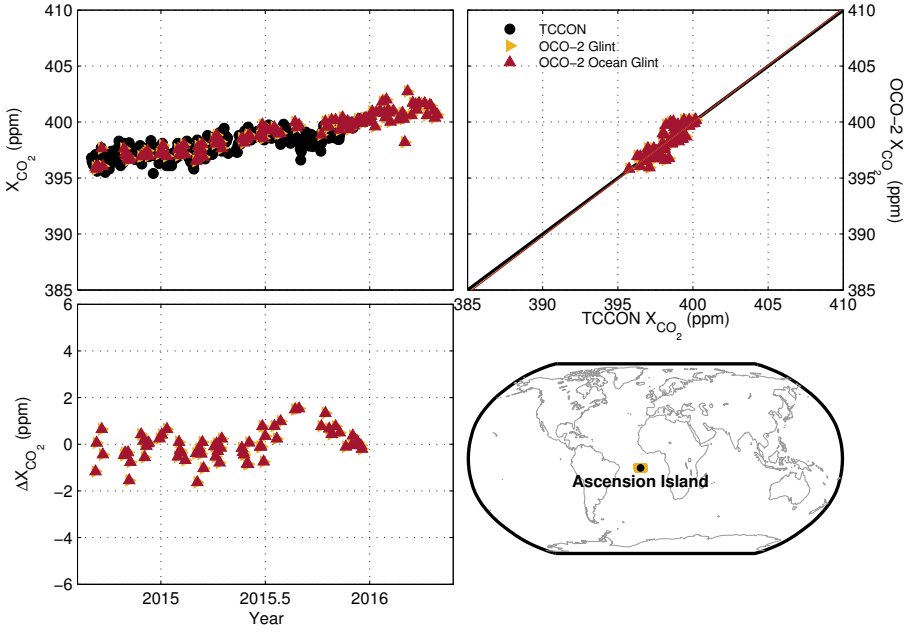

(p) Ascension

Atmos. Meas. Tech. Discuss., doi:10.5194/amt-2016-227, 2016
Manuscript under review for journal Atmos. Meas. Tech.
Published: 29 August 2016

Atmospheric Measurement Techniques Discussions

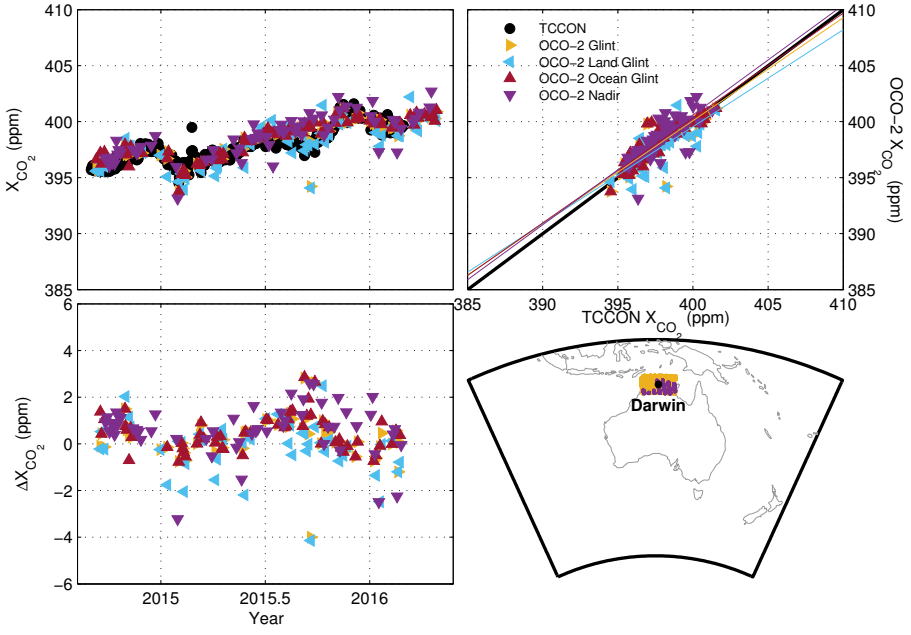

(q) Darwin

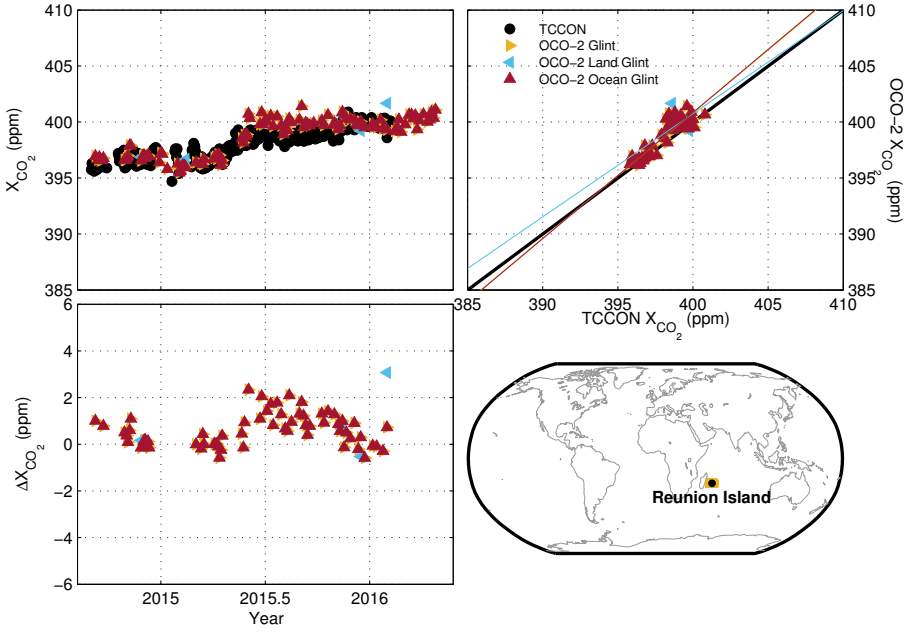

(r) Réunion Island

Atmos. Meas. Tech. Discuss., doi:10.5194/amt-2016-227, 2016
Manuscript under review for journal Atmos. Meas. Tech.
Published: 29 August 2016

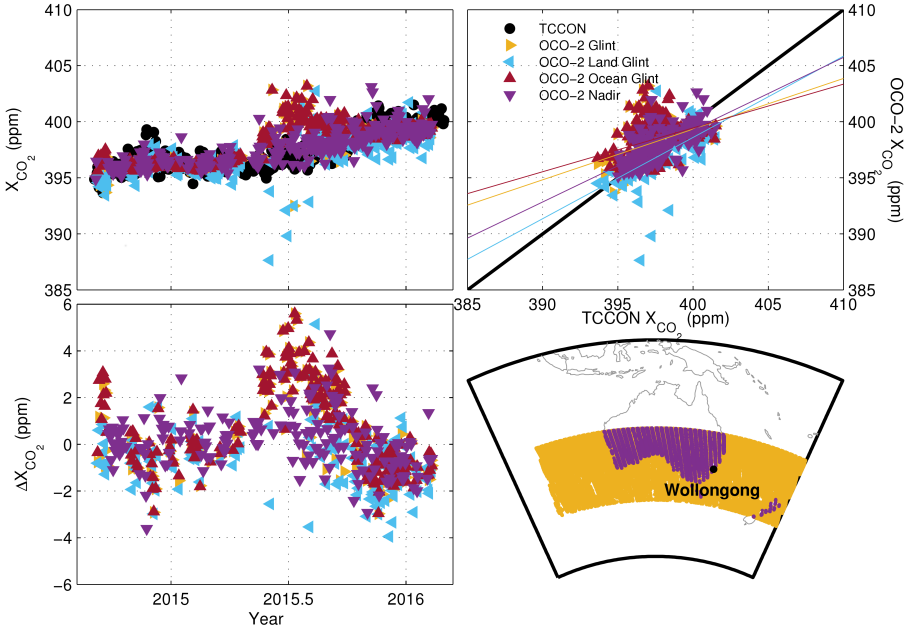

(s) Wollongong

Atmos. Meas. Tech. Discuss., doi:10.5194/amt-2016-227, 2016
Manuscript under review for journal Atmos. Meas. Tech.
Published: 29 August 2016

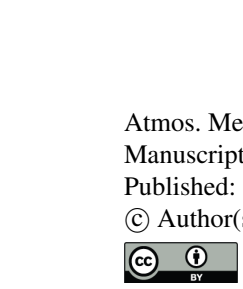

Atmospheric Measurement Techniques Discussions

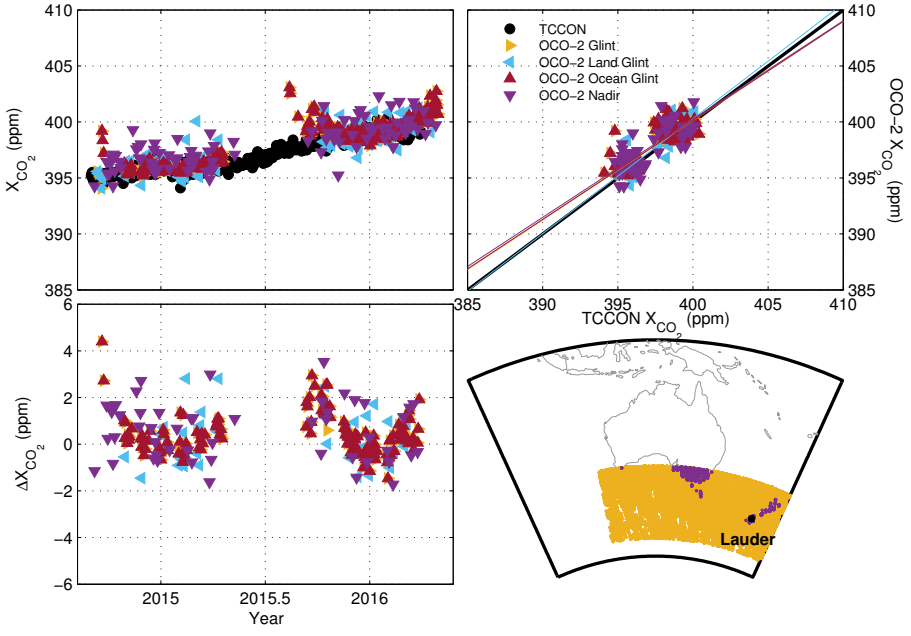

(t) Lauder

Figure A1: The top left panel of each plot (a–t) shows the time series of the TCCON daily medians (black circles), and the daily medians of the OCO-2 glint mode (gold triangles), split into land glint (blue triangles) and ocean glint (red triangles), and OCO-2 nadir mode (purple triangle). The bottom left panel shows the difference between the OCO-2 data and TCCON data as a function of time. The top right panel shows the one-to-one correspondence between the OCO-2 X_{CO_2} values and the TCCON values, and the best fit lines in the colours corresponding to the symbols. The one-to-one line is marked in black. The lower right panel shows the location of the TCCON station (black circle), and the locations of the OCO-2 data, showing glint-mode data in gold and nadir-mode data in purple. The lower right panel is intended to give a sense of the spatial coincidence criteria applied to the OCO-2 data for each TCCON station.

Atmos. Meas. Tech. Discuss., doi:10.5194/amt-2016-227, 2016
Manuscript under review for journal Atmos. Meas. Tech.
Published: 29 August 2016

Atmospheric Measurement Techniques Discussions

Table 1: Available targets. Those available only prior to July 2015 are marked with a natural symbol (♮). Those only available after July 2015 are marked with a sharp symbol (♯). Note that the Target Location may not be exactly centered on a TCCON site location. Targets without a corresponding TCCON station are marked with a flat symbol (♭) and are not discussed in this paper.

Target Name	Target Location (Lat, Lon, Alt)	Target Active Dates	Data Reference
Anmyeondo, South Korea ♯	36.624, 126.373, 0.006	July 2015 - Present	
Ascension Island	-7.947, -14.387, 0.165	July 2014 - Present	Feist et al. (2014)
Białystok, Poland	53.196, 23.0758, 0.124	July 2014 - Present	Deutscher et al. (2014)
Boulder, CO ♭	40.014 , -105.104 , 1.61	July 2015 - Present	
Bremen, Germany	53.104, 8.850, 0.004	July 2014 - Present	Notholt et al. (2014)
Caltech, Pasadena, CA	34.123, -118.073, 0.157	July 2014 - Present	Wennberg et al. (2014c)
ARM TWP - Darwin, Aus	-12.375, 130.917, 0.0049	July 2014 - Present	Griffith et al. (2014a)
Edwards FRC, CA	34.958, -117.882, 0.699	July 2014 - Present	Iraci et al. (2014)
Izaña, Tenerife, Spain	28.297, -16.518, 2.2317	July 2014 - Present	Blumenstock et al. (2014)
Karlsruhe, Germany	49.100, 8.438, 0.11	July 2014 - Present	Hase et al. (2014)
Eureka, Canada ♮	80.053, -86.417, 0.601	July 2014 - June 2015	Strong et al. (2014)
SGP ARM Site, Lamont OK	36.604, -97.486, 0.3179	July 2014 - Present	Wennberg et al. (2014b)
Lauder, NZ	-45.002, 169.685, 0.384	July 2014 - Present	Sherlock et al. (2014)
Libya	28.550, 23.390, 0.108	June 2016 - Present	
Litchfield, Aus	-17.151, 139.795, 0.233	June 2016 - Present	
Manaus, Brazil	-3.213, -60.598, 0.04877	July 2014 - June 2016	Dubey et al. (2014)
Mexico City, Mexico ♭ ♯	19.429, -99.138, 2.239	July 2015 - Present	
Orléans, France	47.965, 2.113, 0.1308	July 2014 - Present	Warneke et al. (2014)
Paris, France ♯	48.846, 2.356, 0.034	July 2015 - Present	Te et al. (2014)
Park Falls, WI	45.945 , -90.273, 0.474	July 2014 - Present	Wennberg et al. (2014a)
Fairbanks, Alaska ♭ ♯	64.859, -147.844, 0.501	July 2015 - Present	
Railroad Valley ♭	38.497, -115.690, 1.4359	July 2014 - Present	
Réunion Island	-21.049, 55.285, 0.504	July 2014 - Present	De Maziere et al. (2014)
Rikubetsu, Japan	43.452, 143.700, 0.236	July 2015 - Present	Morino et al. (2014b)
Rosemount, MN ♭ ♯	44.689, -93.027, 0.289	June 2016 - Present	
Saga, Japan	33.241, 130.288, 0.003	July 2015 - Present	Kawakami et al. (2014)
São Paulo, Brazil ♭ ♯	-23.539, -46.634, 0.76	July 2015 - June 2016	
Shanghai, China ♭ ♯	31.22, 121.456, 0.12	July 2015 - June 2016	
Sodankylä, Finland	67.368, 26.633, 0.18	July 2014 - Present	Kivi et al. (2014)
Tsukuba, Japan	36.051, 140.122 , 0.0277	July 2014 - Present	Morino et al. (2014a)
Wollongong, Aus	-34.451, 150.855, 0.008	July 2014 - Present	Griffith et al. (2014b)

Atmos. Meas. Tech. Discuss., doi:10.5194/amt-2016-227, 2016
Manuscript under review for journal Atmos. Meas. Tech.
Published: 29 August 2016

Atmospheric Measurement Techniques Discussions

Table 2: Filters applied to the target-mode OCO-2 data from the standard OCO-2 files (i.e., not the "lite" files). Parameters for which there is only one limit are marked with a '—'. The units are listed where applicable. The parameter "blended_albedo" is defined as $2.4 \times albedo\_o2\_fph - 1.13 \times albedo\_strong\_co2\_fph$.

Parameter	Lower Bound	Upper Bound	Units
surface_pressure_delta_abp	-4000	583	Pa
retrieval_surface_roughness	—	26.50	
relative_residual_mean_square_weak_co2	—	0.00250	
retrieval_zenith	—	40	°
outcome_flag	—	2	
blended_albedo	—	0.8	
h2o_ratio_idp	0.7	1.02	
co2_ratio_idp	0.995	1.025	
surface_pressure_delta_fph	-5	10	hPa
dof_co2_profile	1.8	—	
ice_aod	—	0.03	
dust_aod	0.001	0.3	
co2_grad_del	-70	70	
sulfate_aod	0.4	—	
albedo_weak_co2_fph	0.1	—	
airmass	—	3.6	
surface_type	'Coxmunk'	'Coxmunk'	

Atmos. Meas. Tech. Discuss., doi:10.5194/amt-2016-227, 2016
Manuscript under review for journal Atmos. Meas. Tech.
Published: 29 August 2016

Atmospheric Measurement Techniques Discussions

Table 3: Glint and nadir statistics. The median bias (OCO-2 - TCCON) and its RMS, R^2 and number of daily median comparison points (N) are listed below for each TCCON station.

	Land Glint				Ocean Glint				Nadir			
TCCON Site	**Bias**	**RMS**	R^2	**N**	**Bias**	**RMS**	R^2	**N**	**Bias**	**RMS**	R^2	**N**
Eureka									0.10	1.99	0.739	3
Sodankylä									3.15	3.21	1.000	2
Białystok	0.29	1.75	0.485	4	0.53	3.57	0.181	3	0.89	1.83	0.766	14
Bremen	1.98	2.36	0.665	4	0.63	0.82	0.903	4	2.27	2.29	1.000	2
Karlsruhe	0.86	1.55	0.676	16					0.96	1.69	0.871	13
Orléans	0.29	2.08	0.369	14	-0.31	2.20	0.256	6	1.15	1.82	0.833	19
Garmisch	0.24	1.00	0.852	11					1.25	2.13	0.528	18
Park Falls	-0.50	1.44	0.919	13	0.60	1.42	0.868	13	0.27	1.55	0.800	19
Rikubetsu	2.64	2.70	0.917	3	1.02	1.10	0.932	4				
Lamont	-0.20	1.23	0.854	52					-0.13	1.18	0.865	81
Tsukuba	0.71	2.47	0.530	6	-0.56	1.79	0.698	16	1.34	3.80	0.288	9
Edwards	-0.08	1.27	0.732	35	-0.13	1.97	0.579	28	0.34	1.17	0.780	51
Pasadena	-0.26	1.20	0.856	5	-1.08	1.79	0.851	3	0.49	0.99	0.929	12
Saga	0.00	1.11	0.916	7	-1.12	1.50	0.715	20	-0.18	0.62	0.936	6
Manaus	-0.82	1.06	0.795	4								
Ascension Island					-0.09	0.63	0.736	66				
Darwin	0.10	0.96	0.676	46	0.40	0.88	0.808	60	0.58	1.04	0.711	56
Réunion Island	0.27	1.16	0.582	4	0.50	0.90	0.824	63				
Wollongong	-0.69	1.40	0.638	154	0.18	2.01	0.183	220	0.03	1.02	0.680	197
Lauder	0.03	0.98	0.731	41	0.27	0.97	0.749	136	0.69	1.30	0.599	51
Total	-0.21	1.36	0.716	419	0.19	1.51	0.501	644	0.29	1.34	0.754	555

Atmos. Meas. Tech. Discuss., doi:10.5194/amt-2016-227, 2016
Manuscript under review for journal Atmos. Meas. Tech.
Published: 29 August 2016

Atmospheric Measurement Techniques Discussions
Open Access
EGU

Table 4: Glint, nadir and target relationships with TCCON. The slope and its uncertainty, R^2 and number of daily median comparison points (N) are listed below for each OCO-2 viewing mode. The values for ocean glint data with and without the southern hemisphere winter data are included on separate rows. Note that the land glint, ocean glint and nadir slopes are computed after the global bias has been removed from the data. The global bias is determined by the target data value listed in the table.

	slope	R^2	**N**
Land Glint	0.9074±0.02	0.72	419
Ocean Glint	0.7167±0.03	0.50	644
Excluding SH Winter	0.8164±0.03	0.71	501
Nadir	0.8690±0.03	0.75	555
Target	0.9975±0.04	0.81	106